iScience

CellPress

Article

A Nanoparticle-Based Affinity Sensor that Identifies and Selects Highly Cytokine-Secreting Cells

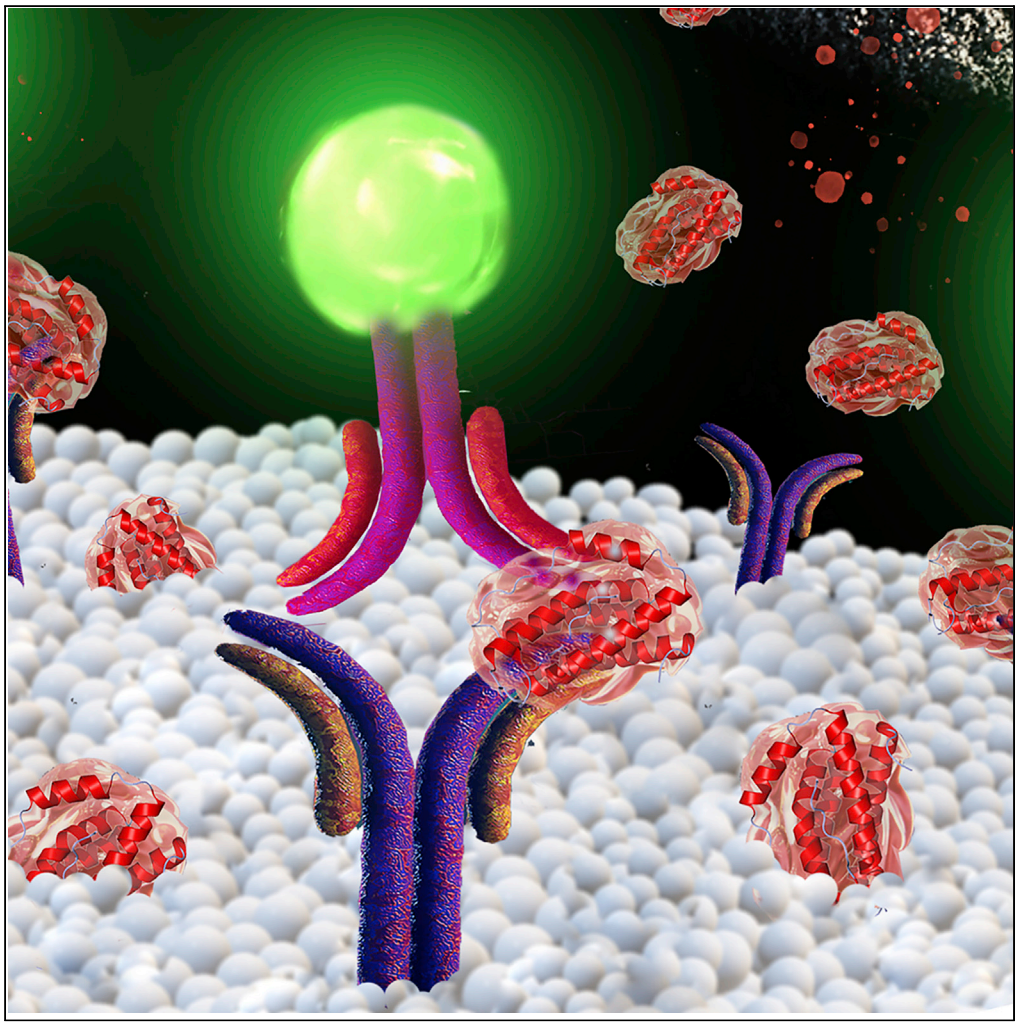

Guozhen Liu, Christina Bursill, Siân P. Cartland, ..., Mary M. Kavurma, Mark R. Hutchinson, Ewa M. Goldys

guozhen.liu@unsw.edu.au (G.L.)
e.goldys@unsw.edu.au (E.M.G.)

HIGHLIGHTS

We developed an assay for detecting cytokine secretion from individual cells

This system is universal to detect different cytokines from a broad range of cell types

The assay can select highly cytokine-secreting cells and purify their populations

This study opens a host of applications for monitoring disease progression

Liu et al., iScience *20*, 137–147
October 25, 2019
https://doi.org/10.1016/j.isci.2019.09.019

iScience

CellPress

Article

A Nanoparticle-Based Affinity Sensor that Identifies and Selects Highly Cytokine-Secreting Cells

Guozhen Liu,[1,2,3,8,*] Christina Bursill,[4,5] Siân P. Cartland,[5,6] Ayad G. Anwer,[1,2] Lindsay M. Parker,[2] Kaixin Zhang,[2] Shilun Feng,[2] Meng He,[2] David W. Inglis,[2] Mary M. Kavurma,[5,6] Mark R. Hutchinson,[7] and Ewa M. Goldys[1,2,*]

SUMMARY

We developed a universal method termed OnCELISA to detect cytokine secretion from individual cells by applying a capture technology on the cell membrane. OnCELISA uses fluorescent magnetic nanoparticles as assay reporters that enable detection on a single-cell level in microscopy and flow cytometry and fluorimetry in cell ensembles. This system is flexible and can be modified to detect different cytokines from a broad range of cytokine-secreting cells. Using OnCELISA we have been able to select and sort highly cytokine-secreting cells and identify cytokine-secreting expression profiles of different cell populations *in vitro* and *ex vivo*. We show that this system can be used for ultrasensitive monitoring of cytokines in the complex biological environment of atherosclerosis that contains multiple cell types. The ability to identify and select cell populations based on their cytokine expression characteristics is valuable in a host of applications that require the monitoring of disease progression.

INTRODUCTION

Probing how cells secrete cytokines as they respond to the surrounding signals is a major challenge (Liu et al., 2016; Zhao et al., 2011). Given the important roles of cytokines across the biological spectrum, including the control of cell replication and apoptosis, cancer, atherosclerosis, and tissue regeneration and in the modulation of immune reactions (Müller et al., 2002; Nicola, 1994), it is critical to advance the understanding of the heterogeneity of cellular cytokine release at the level of single cells (Bienvenu et al., 2000). This inspired us to create a simple and sensitive single-cell cytokine analysis platform that enables a nuanced characterization of individual cytokine-secreting cells as well as quantitative analysis of cytokines secreted from each cell. Our new approach is sensitive; it does not appreciably affect cell secretion, and labeled cells are able to proliferate.

The current leading approach for cytokine detection is enzyme-linked immunosorbent assays (ELISA), which detects average cytokine concentration in solutions of culture media, blood, plasma, synovial fluid, or homogenized cell lysates or tissues, typically in the picomolar range (Schenk et al., 2001). An example commercial assay (Achard et al., 2003) detects mouse interleukin (IL)-6 cytokine with a sensitivity of 18.2 pg mL^{-1} in a 5-μL sample, whereas a high-throughput multiplex Illumina technology detects a panel of 96 cytokines at concentrations from 0.5 pg mL^{-1} to 14 pg mL^{-1} in 50-μL samples (Quinn et al., 2008). These assays cannot detect specific cytokine secretions from single cells and only provide information about the average cytokine concentration, which reflects the total expression over time (dependent on the stability of the measured protein). Cellular cytokine assays typically use intracellular transport inhibitors such as brefeldin A (Biosciences), which prevent cytokine release, and consequently kill the cells, considerably limiting the scope of their application. Inhibitor-free technologies (Brosterhus et al., 1999; Wilson et al., 2007) have only been demonstrated in T cells.

Here, we present a universal approach to highly sensitive detection of trace cytokine secretions from individual, single live cells, which we call "OnCELISA." Our OnCELISA assay extends the ELISA approach by utilizing the cell surface to capture the secreted molecules where they can be detected by fluorescent labeling. Such cell-surface affinity sensors have been previously used to detect antigen binding (Rider et al., 2003), ATP release (Beigi et al., 1999), the presence of growth factors (Zhao et al., 2011), abundant cytokines (Holmes and Al-Rubeai, 1999; Manz et al., 1995), and other targets (Ali et al., 2012; Jiang et al., 2015). We have been able to create capture surfaces on cell membranes that do not affect cell secretion and enable proliferation. Transcending the previously published work, we have been able to introduce fluorescent

[1]Graduate School of Biomedical Engineering, ARC Centre of Excellence in Nanoscale Biophotonics (CNBP), Faculty of Engineering, The University of New South Wales, Sydney, NSW 2052, Australia

[2]ARC Centre of Excellence in Nanoscale Biophotonics (CNBP), Macquarie University, Sydney, NSW 2109, Australia

[3]International Joint Research Center for Intelligent Biosensor Technology and Health, College of Chemistry, Central China Normal University, Wuhan 430079, P. R. China

[4]Heart Health Theme, South Australian Health and Medical Research Institute, Adelaide, SA 5005, Australia

[5]Heart Research Institute, Sydney 2042, Australia

[6]Sydney Medical School, University of Sydney, Sydney, Australia

[7]ARC Centre of Excellence in Nanoscale Biophotonics (CNBP), School of Medicine, Adelaide University, Adelaide, SA 5005, Australia

[8]Lead Contact

*Correspondence: guozhen.liu@unsw.edu.au (G.L.), e.goldys@unsw.edu.au (E.M.G.)

https://doi.org/10.1016/j.isci.2019.09.019

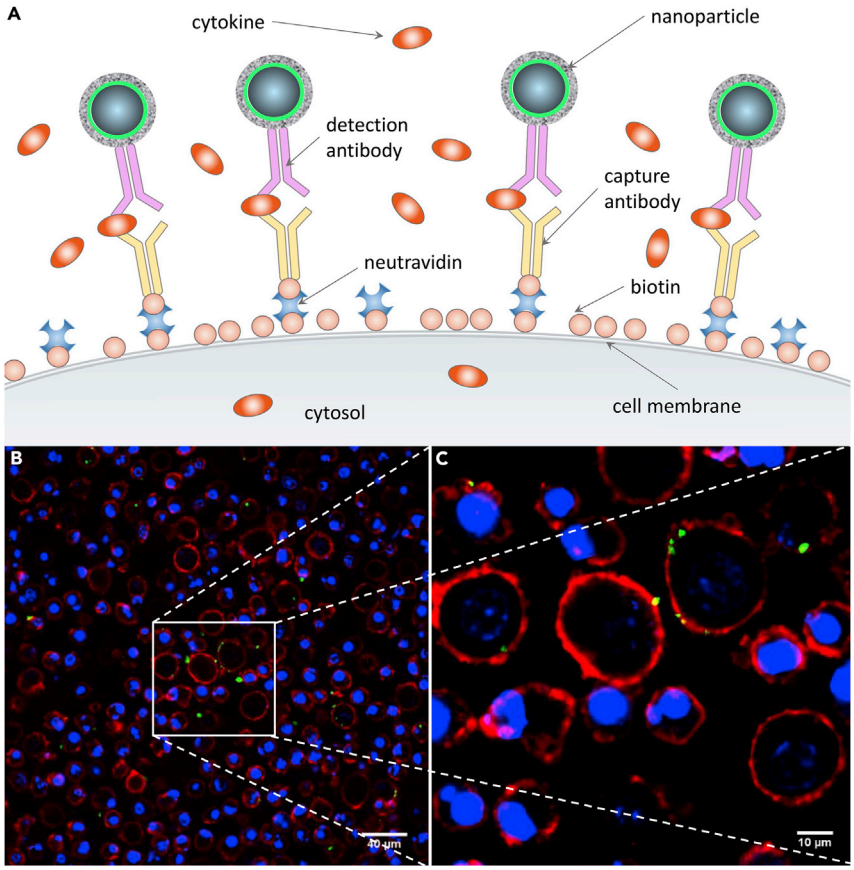

Figure 1. OnCELISA Assay

(A) Assay schematics where magnetic fluorescent nanoparticles are captured by antibodies on the biotinylated surface of cells. (B and C) Assay implementation in RAW cells shown by confocal laser scanning microscopic images at two magnifications. Green indicates successful OnCELISA labeling with fluorescent magnetic nanoparticles; blue, Hoechst; red, cell mask deep red membrane staining.

magnetic nanoparticles as assay reporters. This enhances the sensitivity of OnCELISA to 0.1 pg mL^{-1}, which is 10-fold more sensitive than with standard fluorophore labels. Our assay uniquely combines the advantages of both cell-surface affinity capture (Kenney et al., 1995) and magnetic cell sorting/separation (Tibbe et al., 2002). Using mathematical modeling and single-cell experiments, we confirmed that OnCELISA predominantly detects cytokine secretions from the same cell where they were captured.

With these new capabilities of OnCELISA we were able (1) to assess the ability of individual cells to secrete cytokines, (2) to distinguish highly secreting cells from poorly secreting ones, and (3) aided by fluorescence *in situ* hybridization labeling of the relevant messenger RNA, to provide insights into the cytokine secretion dynamics, in particular on the existence of early and late responders to cytokine stimulation. Furthermore, brightly fluorescent OnCELISA magnetic bead labeling made it possible to detect the *ex vivo* secretion of IL-6 from multi-cellular atherosclerotic plaque-containing mouse aortae. OnCELISA *ex vivo* was responsive to an inflammatory stimulus and to an increase in the stage of atherosclerotic disease development. The capability to select cells with a range of cytokine secretion levels and the ability to purify cell populations through identification of cellular expression levels on a single-cell basis may have significant implications for future cell therapy applications and for tracking disease progression in preclinical models.

RESULTS

Engineering and Testing the Cell-Surface Cytokine OnCELISA Assay

We designed our cytokine capture surface as shown in Figure 1A. In our approach, cells first undergo surface biotinylation followed by the attachment of neutravidin and a biotinylated IL-6 capture antibody to

form the capture surface (Holmes and Al-Rubeai, 1999). The capture surface enables the cytokine molecules secreted by cells to be immobilized on the cell surface immediately upon their release, before they become diluted in the medium. These captured cytokines are then visualized by fluorescent magnetic particles functionalized with detection antibodies. Their fluorescence signal indicates the amount of cytokine secretion (Figures 1B and 1C) (see Transparent Methods). The two antibodies required for OnCELISA (capture and detection) are raised to different epitopes of the target cytokine. Importantly, as we show later, the cells are not affected and can be cultured after the application of OnCELISA.

The design of the OnCELISA affinity surface was verified by using BV2 microglial cells. Figures S1A–S1C show that the capture antibody is uniformly distributed on the cell surface. The IL-6 detection antibody conjugated to fluorescent magnetic nanoparticles (Dragon Green superparamagnetic iron oxide, DG SPIO) via amide bonds displays similar fluorescence as the unconjugated DG SPIO (Figure S1D). The attachment of antibodies to the fluorescent magnetic nanoparticles was further confirmed by their increased hydrodynamic size (951 $\pm$ 15 nm before and 989 $\pm$ 10 nm after conjugation) and by zeta-potential measurements (Figure S2). The DG SPIO-conjugated IL-6 antibodies (DG SPIO IL-6 Ab) retain their affinity to IL-6 upon conjugation as seen in Figure S3A. The calibration curve in Figure S3B indicates that the OnCELISA assay with fluorimetry readout is able to detect IL-6 down to 0.1 pg mL^{-1}, with a linear range between 0.1 and 1,000 pg mL^{-1}.For comparison, the low detection limit of mouse IL-6 in a BD OptEIA ELISA kit is 3.8 pg mL^{-1}, whereas the Cisbio Bioassays product can detect 18.2 pg mL^{-1}(Achard et al., 2003). The assay design was additionally confirmed using lipopolysaccharide (LPS) stimulation, as shown in Figure S4 where we also verified negligible (5%) non-specific adsorption and/or uptake of the DG SPIO IL-6 Ab particles (see Table S1 for a summary of control experiments). Figures S5 and S6 show the location of OnCELISA labeling, mostly on cell surface, with some cell-type-dependent nanoparticle uptake occurring after labeling, which does not affect the assay reading (Betzer et al., 2015). The OnCELISA labeling of cells was stable after 12 h at 4°C. All these characterizations indicate that the level of OnCELISA labeling reflects the level of cytokine secretion from each cell.

Cytokine Secretion from BV2 Cells following Cell Stimulation with Lipopolysaccharide

We characterized IL-6 cytokine secretion from the BV2 cell line by OnCELISA following LPS stimulation (Figures 2A–2C). Figure 2B shows that only some cells were labeled by OnCELISA, which may indicate that only this portion of cells were expressing high enough amounts of IL-6. The results of fluorescent *in situ* hybridization of the IL-6 mRNA expression (Figures 2E–2G) also indicate variable expression of IL-6 mRNA in different cells. We verified that the affinity surface on a cell preferentially captures IL-6 from this cell and not from the solution. To show this, OnCELISA was applied to cells with the capture surface antibody as in Figure 1A, but without LPS stimulation. A high concentration of IL-6 of 200 pg mL^{-1} (100 times higher than the concentration of IL-6 in body fluids) was then spiked into the medium, following by the DG SPIO_IL-6_Ab. No labeling on the cell surface was observed in microscopic imaging (Figure 2D). This is consistent with the IL-6 capture antibody on the surface of a cell preferentially capturing the IL-6 molecules from this particular cell immediately after secretion. The capture occurs when the IL-6 molecules are still present in high concentration near the cell membrane, before they diffuse away. This was confirmed using mathematical modeling of OnCELISA (see Transparent Methods for vesicular model of cytokine release). These features of the OnCELISA assay make it possible to differentiate cells secreting high amounts of IL-6 from poorly secreting cells. Furthermore, we used OnCELISA to monitor the time course of cytokine secretion in functionalized cells stimulated by LPS. The presence of IL-6 released by the cells into the cell culture medium was consistent with the results of our IL-6 mRNA assay (Figures 2E and 2F) and confirmed by a standard ELISA assay (Figure 2H). Both ELISA and OnCELISA indicate that IL-6 secretion by BV2 cells (for cell density of 2.0 $\times$ 10^6 +/− 0.16 cells per mL) increased with the LPS stimulation time, and a maximum level of IL-6 (~493 pg/mL) was obtained with LPS stimulation for 8 h, thereby further validating OnCELISA. The secretion rate was constant in the first 4 h, estimated to be 0.6 $\pm$ 0.2 molecule/s per cell (Figure 2H).

Next, we carried out the OnCELISA assay in a microfluidic chip in which each cell is located in an individual well, separated from its neighbor by a distance of 25 μm. The percentage of the OnCELISA-labeled cells was 38% $\pm$ 8%, similar to the labeled fraction in suspended cells discussed below (example results are shown in Figure 2I). Using this chip we also verified that OnCELISA labeling was observed in the cells that are simultaneously labeled for IL-6 mRNA (Figures 2E–2G). We found that, generally, more cells were positive for IL-6 mRNA expression than for IL-6 OnCELISA with 2-h LPS stimulation. This is consistent

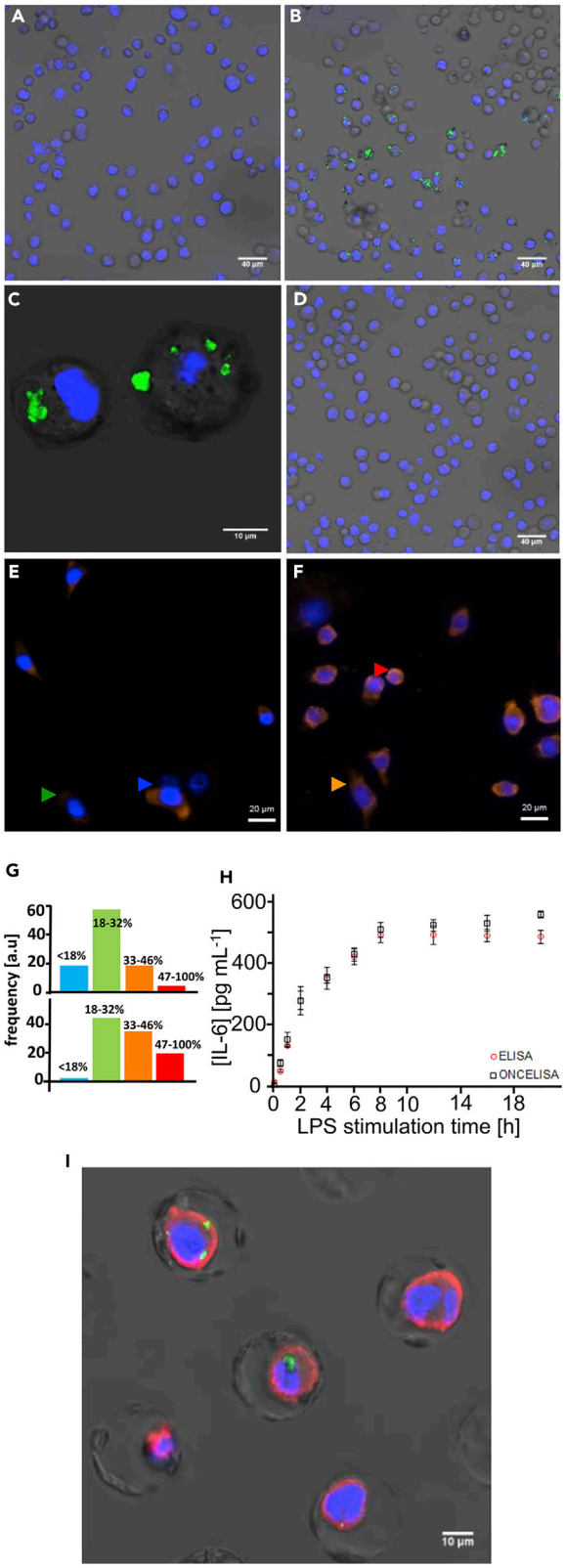
A
B
C
D
E
F
G
H
I
frequency [a.u]
<18%
18-32%
33-46%
47-100%
[IL-6] [pg mL-1]
ELISA
ONCELISA
LPS stimulation time [h]
10 µm
20 µm
40 µm

Figure 2. Characterization of LPS-Stimulated BV2 Cells

(A–D) Combined differential interference contrast (DIC) and confocal laser scanning microscopy images of BV2 cells incubated with OnCELISA labeling (with nucleus Hoechst staining in blue) after 8-h LPS stimulation, before (A) and after treatment (B and C) with DG SPIO_IL-6_Ab (green) at different magnifications; (D) functionalized cells without LPS stimulation after spiking 200 pg mL^{-1} IL-6 to the medium solution followed by adding the DG SPIO_IL-6_Ab.

(E and F) IL-6 mRNA expression in BV2 cells detected by fluorescence *in situ* hybridization staining (orange, AlexFluor 555; blue, DAPI nuclear stain). Cells were incubated with biotin-incorporated IL-6 cRNA probes at 0 h (E) and 2 h (F) following LPS stimulation and labeled by streptavidin-AlexaFluor 555 IL-6. At both time points, the cells were expressing varying levels of mRNA (very low expression, blue arrow; low expression, green arrow; high expression, orange arrow; very high expression, red arrow).

(G) Fluorescence intensity histograms (from over 1,000 cells) of mRNA expression in these four classes of cells for 0 h LPS (top) and 2 h LPS (bottom), with relative brightness limits indicated in the figure.

(H and I) (H) ELISA of IL-6 for cells after LPS stimulation for different periods of time, and fluorescence intensity for DG SPIO_IL-6_Ab-labeled cells (OnCELISA) with LPS stimulation for different periods of time (data between 9 and 20 h was not collected because of no laboratory access at midnight); (I) combined DIC and confocal laser scanning images of a single-cell chip with wells holding individual cells stained for nuclei (blue, Hoechst), IL-6 mRNA (red), and OnCELISA (green).

with the expression of IL-6 mRNA being only one of many rate-limiting steps in the process of cellular expression of the IL-6 protein.

Mathematical Modeling Predicts That OnCELISA on a Single Cell Preferentially Detects Own Secreted Cytokine Molecules

We explored whether the OnCELISA assay on a specific cell captures the cytokines that originate from that particular cell or cytokines secreted by adjacent cells. To this aim, we developed a mathematical model of cytokine secretion from cells (Lacy and Stow, 2011) (see Transparent Methods for details). The model assumes that the cytokines are released from small (<1 μm) secretory vesicles composed of a high (millimolar range) concentration of cytokines (Stow et al., 2009). Once released, the cytokines form a hemispherical cloud of molecules diffusing away from the cell, with a radius of $R = \sqrt{Dt}$. Here D is the diffusion constant and t is time since the moment of vesicle rupture. The model makes it possible to estimate the local cytokine concentration at the cell surface, which is transiently much higher than the average in the medium. The interaction of cytokines released from the vesicles is further described using conventional chemical kinetics to evaluate the time constant for the cytokine-binding reaction. The results suggest that the cytokine reaction kinetics is very fast, because the OnCELISA capture surface is on the cell membrane, where the cytokine release produces a transiently high cytokine concentration. In our experimental conditions, we estimate that the binding time constant of 0.4–1.6 s and 63% achievable binding to the affinity surface will take place in the region of radius of 1.3–2.0 μm from the ruptured vesicle. This means that OnCELISA on a cell that is isolated from other cells by more than 2 μm detects only its own cytokines.

OnCELISA-Labeled Highly Cytokine-Secreting Cells Form a Clear Subpopulation that Can Be Purified

We further demonstrated that the OnCELISA assay is compatible with flow cytometry, so it may be used for rapidly screening large numbers of cells, distinguishing cell subpopulations, and selecting target cells (Foster et al., 2007). The OnCELISA assay was applied to BV2 cells, and a subsequent flow cytometry measurement showed that the OnCELISA clearly labels the cells into a distinguishable population, as shown in Figure 3B, with 38% of the cells in the DG SPIO_IL-6_Ab population. However, the control cells which were treated with OnCELISA but without the attachment of biotinylated anti IL-6 Ab, did not show the cell population with the fluorescence labelling (Figure 3A). No OnCELISA labelling was observed in the confocal imaging of the control cells either (Figure 3C). We have also shown that OnCELISA is compatible with an alternative cell selection methodology, magnetic sorting. Starting from the same LPS-stimulated BV2 cells we were able to select the OnCELISA-labeled subpopulation with a magnetic pen (see Transparent Methods). As shown in Figures 3D and 3F the OnCELISA labeling efficiency (percentage labeled cells) and hence detectable cytokine-secreting cells is about 32% ± 8%, consistent with the values obtained by flow cytometry and with single-cell chip data 38% ± 8% (Figure 2I). The OnCELISA labeling efficiency increased to about 72% ± 8% after magnetic sorting (Figures 3E and 3F). Thus, the majority of the labeled cells can be sorted by flow cytometry or by magnetic sorting.

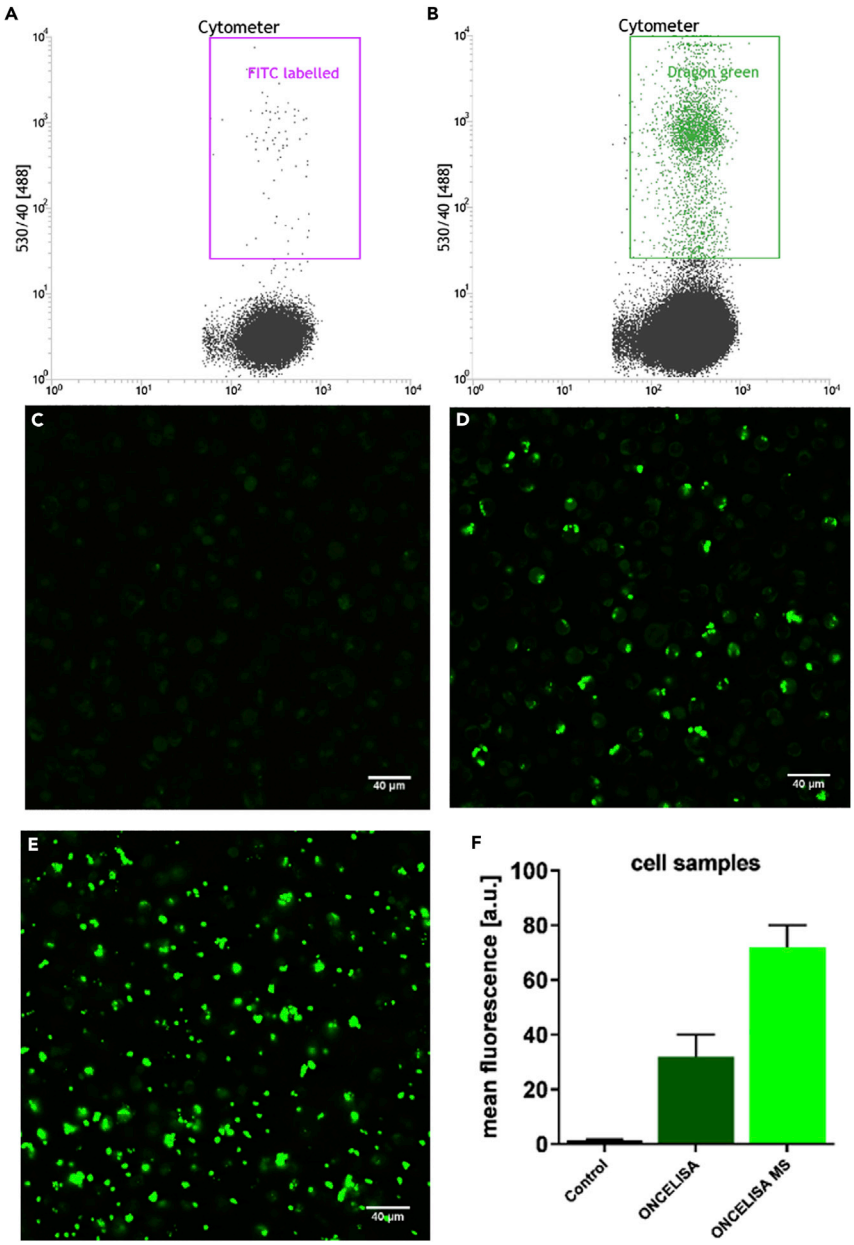

Figure 3. OnCELISA Labeling of LPS-Stimulated BV2 Cells

(A–F) Flow cytometry results for (A) control and (B) cells labeled with DG SPIO_IL-6_Ab (OnCELISA). Confocal laser scanning microscopy images for (C) control, (D) cells labeled with OnCELISA after treatment with LPS, (E) cells selected out after application of magnetic sorting, and (F) the fluorescent count of control and cells labeled with OnCELISA before and after magnetic sorting.

The Progeny of Sorted, Highly Secreting Cells Inherits High Secretion

The OnCELISA-labeled magnetically sorted BV-2 cells were cultured further to establish cell viability and proliferation potential. Figures 4A and 4B confirm that cells labeled with DG SPIO_IL-6_Ab can proliferate, as apparent from the formation of a cell cluster. The sorted cells were then cultured, and the OnCELISA labeling was applied again, as described in Transparent Methods. Using a fluorescein isothiocyanate (FITC)-avidin assay we verified that the progeny of the sorted cells remained (partly) biotinylated (Figure S7). Figure 4C shows the confocal images of the OnCELISA-labeled progeny of the previously sorted cells. The labeling efficiency was 59% ± 8%, which is much higher than the 32% ± 8% observed in the unsorted cells. This result indicates that

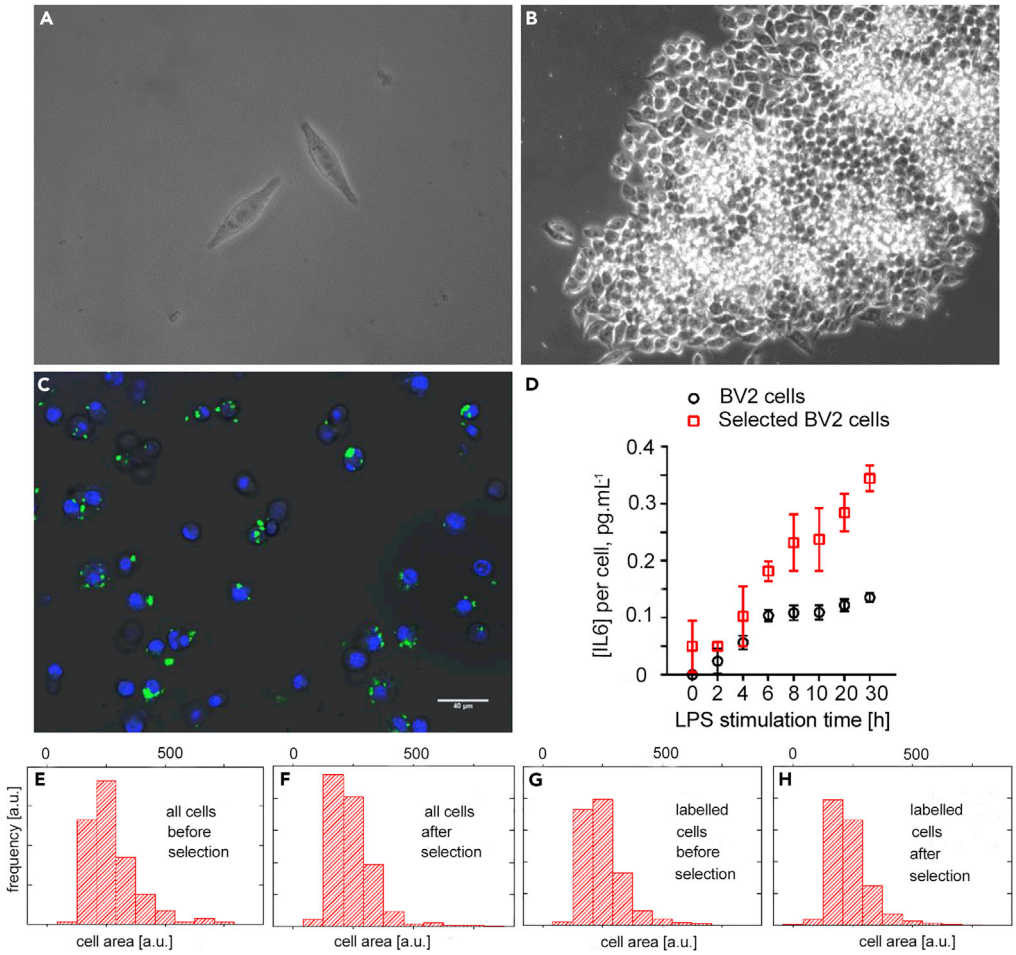

Figure 4. Differential Interference Contrast (DIC) Microscopy Images of Sorted BV2 Cells after Incubation with OnCELISA

(A) 3 days and (B) 7 days; (C) combined DIC and confocal laser scanning microscopy images of Dragon Green SPIO_IL-6_Ab-labeled progeny of highly cytokine-secreting BV2 cells previously magnetically selected using OnCELISA. The progeny cells have grown for 7 days after magnetic selection, and they were biotinylated again before labeling.
(D) Changes in IL-6 concentration with LPS stimulation time for all BV2 cells and OnCELISA-selected BV2 cells.
(E–H) Histograms of cell area for all BV2 cells and OnCELISA-labeled BV2 cells before and after magnetic selection. The x and y axes of (E–H) are the same.

the capacity of the cells to secrete high levels of IL-6 is inheritable. The retention of high IL-6 secretion was also confirmed by ELISA. Figure 4D shows that the IL-6 concentration secreted by the selected BV2 cells is about twice that of the BV2 cells before selection, in close agreement with the OnCELISA labeling ratio. Interestingly, the selected BV2 cells can secrete IL-6 (~0.04 pg mL^{-1} per cell) without LPS stimulation. The OnCELISA-positive cell subpopulation before and after selection was additionally characterized to document whether biological differences exist with unsorted cells. Figures 4F and 4H show that the size histogram of the selected cells shows a higher proportion of small cells compared with the histogram before the selection (Figure 4E, 4G). This means that OnCELISA does not select senescent cells that are typically larger (Childs et al., 2015; Starr et al., 2009), but may select the smaller and younger cells.

Universal OnCELISA that Is Applicable to Other Cell Types and to Other Secreted Products and Can Simultaneously Detect More than One Cytokine

To present a proof of concept of wide applicability of OnCELISA we applied the assay to other cell types and other secreted proteins. To this aim, we prepared the IL-6 capture surface shown in Figure 1 on RAW cells and on adipose-derived mesenchymal stem cells (MSCs). The results of the OnCELISA assay for these

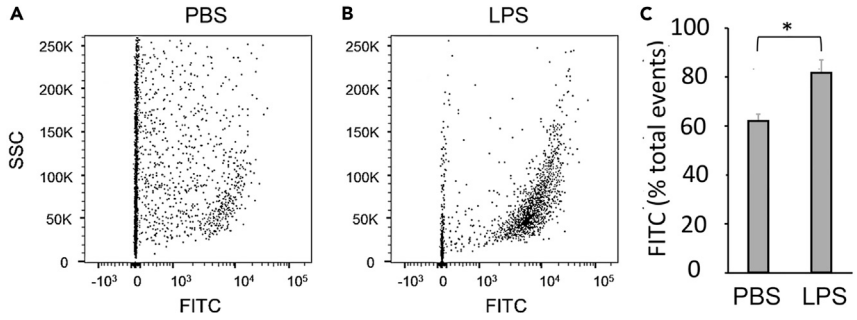

Figure 5. Detection of IL-6 Using OnCELISA in Atherosclerotic Plaque-Containing Mouse Aortae

Apolipoprotein $E^{-/-}$ mice were fed a standard chow diet for 16 weeks to promote atherosclerotic plaque development in their aortae. Excised aortae were digested into single-cell suspensions, and flow cytometry was used to detect the number of viable IL-6-expressing (FITC-positive) cells. (A and B) Dot blots gated on viable cell number demonstrating the presence FITC-positive aortic cells following incubation with (A) phosphate-buffered saline (PBS) or (B) LPS and (C) the change in FITC signal with LPS treatment. * denotes statistical significance, $p < 0.06$.

cells are shown in Figures 1B, 1C, and S8. Owing to lower IL-6 secretion, the level of OnCELISA labeling for these two types of cell lines was lower than that for the BV2 cells (Figure S9). We have also tested that OnCELISA can detect the secretion of another important cytokine, IL-1β (Figure S10). In addition, we verified that OnCELISA can be simultaneously used with two different color particles and two cytokines (Figure S11). The ability of OnCELISA to detect more than a single cytokine is important as cytokines often work synergistically (Kulbe et al., 2012).

OnCELISA Detecting Cytokine IL-6 from Aortic Cells in a Murine Model of Atherosclerosis

We next demonstrated that OnCELISA could be used for the detection of cytokine IL-6 secreted *ex vivo* from multi-cellular aortae containing atherosclerotic plaque. Atherosclerosis is an inflammatory-driven disease characterized by the deposits of inflammatory cells within the artery wall. The apolipoprotein $E^{-/-}$ mouse spontaneously develop atherosclerotic plaques in their aortae. OnCELISA provided robust detection of IL-6 using flow cytometry (FITC-positive cells) in single-cell suspensions of digested plaque-containing aortic tissue. In accordance with an increase in inflammation, more aortic cells were found to be FITC positive following stimulation with LPS in aortae from mice (Figures 5A–5C), when compared with phosphate-buffered saline non-stimulated control aortae.

DISCUSSION

Cytokines secreted from cells play a critical role in controlling cell survival, growth, migration, development, differentiation, and function by binding with specific cytokine receptors and initiating their complex signaling events (Hafler, 2007; Whicher and Evans, 1990; Young, 2009). They are heterogeneously released, creating a unique signaling microenvironment around the reactive and responding cells (Schenk et al., 2001). At the cellular level, a few secreted cytokine molecules may be sufficient to induce a significant cellular response (Gurevich et al., 2003). This strength of the cytokine effect causes the study of cytokine secretion to be experimentally challenging (Stenken and Poschenrieder, 2015), even more so that they are soluble proteins that once released from the cell diffuse away and become diluted in culture media, blood, or other tissue fluids, depending on the site of secretion.

Current single-cell analysis methods capable of analyzing secreted products include enzyme-linked immune absorbent spot (ELISPOT) (Streeck et al., 2009), droplet cytometry (Joensson and Svahn, 2012), encapsulation in microbeads (Turcanu and Williams, 2001), microengraving (Love et al., 2006), and single-cell barcode microchip (Fan et al., 2008). Their disadvantages were discussed in Han et al. (2010). In particular, in ELISPOT the cells are sparsely spread over a surface with immobilized capture antibodies and immobilized secretion products detected by a colorimetric reaction. In this approach accuracy is limited as individual spots may overlap or single cells may cluster. Furthermore, the cells are lost during the process (Han et al., 2010). Droplet cytometry (Joensson and Svahn, 2012), wherein cells are individually contained and analyzed in droplets, is not capable for absolute quantification of secreted proteins owing to the lack of calibration approaches and challenges in loading single cells (Han et al., 2010). Encapsulation in microbeads (Turcanu and Williams, 2001) may introduce cross-contamination among cells, may perturb secretion (as cells may need to be cooled to 4° to achieve agarose

gelling), and requires additional processing to recover cells (Han et al., 2010). Microengraving introduced in Love et al. (2006) isolates individual cells in a dense, elastomeric array of custom-made microwells (~100 pL). The microwells are then sealed by glass slides coated with capture reagents. The slides undergo postprocessing with detection reagents and are read out by a fluorescent scanner. Microengraving requires careful manipulation of glass slides so that there is no cross-contamination of detection spots with fluid from adjacent wells, or without stimulating or dislodging single cells. Its low throughput and difficulties of automation have limited its widespread adoption. Single-cell barcode microchips (Fan et al., 2008) use custom-made microfluidic microchambers pre-printed with antibodies. Cell delivery and deposition in wells is challenging, and the system has low throughput. Intracellular staining (Jung et al., 1993) blocks cytokine secretion, and cells cannot be analyzed when live as membrane permeabilization is required. The cell is tested when prohibited from secretion, which may not accurately reflect secretion of a live cell. In contrast to these methods, OnCELISA does not require custom-made microfluidics and only uses commercially available reagents. Cells are tested live, and they do not require postprocessing to be able to proliferate. The method is fully compatible with flow cytometry, enabling cell selection. Quantification of secreted products and calibration is also possible.

The cellular secretion assay presented here, uses fluorescence detection so that the cells can be interrogated individually by fluorescence microscopy, flow cytometry, or as an ensemble by fluorimetry. The accuracy of OnCELISA analysis on a single-cell level is affected by any variation in biotinylation of live cells, anchoring of capture probes, cytokine binding, and secondary reporter binding. The extent of these variations is reflected in the size of error bars in Figure S3B, where OnCELISA was applied to exact replicates of cell ensembles at a number of IL-6 concentrations introduced by spiking. It shows that the assay reproducibility is high, with average variation of 11%.

Low number of copies of individual target molecules combined with the unavoidable presence of cellular autofluorescence background pose a challenge for fluorescence detection, which can be addressed by using bright labeling or amplification (Lei and Ju, 2012). In this work, we chose to use bright and relatively large (few hundred nanometers) nanoparticle labels (Deng and Goldys, 2014). Owing to the brightness of our labels, the OnCELISA assay is sensitive enough (0.1 pg/mL) to detect cytokines secreted by single cells. This is an advance over standard single-cell analysis method such as microengraving where conventional sandwich immunofluorescence detection offers sensitivity of ~1 ng/mL, or 10 pM, for most soluble proteins (Herrera et al., 2019) (for example, Love et al., 2006, reports the lowest detected cytokine concentration to be 4 ng/mL). Recently, microengraving with quantum dot (QD) nanomaterials as assay reporters, chemical amplification (more than one QD per antibody), and single-particle counting achieved the limit of detection of 60 aM for tumor necrosis factor-α (Herrera et al., 2019). This is about two orders of magnitude lower than reported in this work, pointing to possible improvements in the OnCELISA assay where chemical amplification and single-particle counting can also be applied.

Being able to probe how the individual cells secrete cytokines makes it possible to detect how they respond to the surrounding signals such as LPS stimulation, on the relevant timescale of several hours. Our results shown in Figure 2H make it possible to calculate the secretion frequency from single BV2 cells in the first 4 h when the secretion rates were approximately constant. We obtained secretion rates of 0.6 ± 0.2 molecules/s per cell. This corresponds closely to the cellular IL-6 secretion rate of 0.5 molecules/s per cell reported in Han et al. (2010) for peripheral blood mononuclear cells. Close similarity of these values lends support to the argument that cytokine secretion rates are not affected by the OnCELISA processing of cells. The flexibility of simultaneous monitoring of multiple secreted cytokines (IL-6 and IL-1β) provides an exciting opportunity to explore the "immune synapse" in far greater detail than previously possible.

Importantly, our design only uses commercially available reagents, so it can be easily reproduced in other laboratories. Its universal capture surface is applicable to various cytokines (here, IL-6 and IL1-β) and is potentially suitable for a broad range of cell types (including BV2, RAW, and MSC cell lines presented here) that secrete cytokines or other protein. OnCELISA also demonstrated robust *ex vivo* detection of IL-6 secretion from the aortae of mice that contained atherosclerotic plaque. Atherosclerotic plaque is a complex biological environment that contains multiple cell types. OnCELISA was able to be used on plaque-containing aortae digested into a single-cell suspension to capture and detect the expression of IL-6 from a multi-cellular environment, without the need prepare a cell homogenate as current commercial ELISAs do. This enables the unique capability to characterize the different cells further, whether it be in functional assays or using confocal microscopy, for example.

The immunosensing scheme in this work uses a sandwich immunoassay, similar to a range of commercial ELISA systems. Our approach may make it possible to make these standard ELISA assays more sensitive and convert them into the OnCELISA format. Selection of high cytokine-producing cell populations is an important first step in the characterization of the mechanisms underpinning critical heterogeneity in cytokine signaling. The capability to select highly cytokine-expressing cells in complex biological diseases is also valuable for future cellular therapies using cells selected to optimize their specific properties. Such populations may also be therapeutically useful, for example, by interfering with the opposite immune response near the diseased site. Such selected cell populations have traditionally been delivered by rounds of limiting dilution cloning, followed by product analysis. However, these methods are labor intensive, costly, time consuming, and have low efficiency. In contrast, our OnCELISA assay, which detects and measures single-cell secretion of specific cytokines using fluorescent magnetic particles, makes it possible to select cells with optimized cytokine secretion rapidly and efficiently.

Limitations of the Study

The OnCELISA method presented here is able to probe how individual cells secrete cytokines as they respond to the environmental cues. In addition, the OnCELISA method has the capacity for simultaneously testing the secretion of multiple cytokines, demonstrated using two cytokines IL-6 and IL-1β. Our system can be used for ultrasensitive monitoring of cytokines in the complex biological environment of atherosclerosis that contains multiple cell types. We believe this study will be of interest to a broad community of researchers from areas of cell biology to oncology. In this study the cells did not perform to the internalization of capture antibodies attached to the cell surface. We cannot rule out the possibility that the attached capture antibodies were internalized by certain cell types. To provide further evidence of non-antibody internalization of capture antibodies, validation of OnCELISA using a spectrum of cell types would be required.

METHODS

All methods can be found in the accompanying Transparent Methods supplemental file.

SUPPLEMENTAL INFORMATION

Supplemental Information can be found online at https://doi.org/10.1016/j.isci.2019.09.019.

ACKNOWLEDGMENTS

This work was financially supported by funding from the ARC Future Fellowship (FT160100039 to G.L.), the ARC Center of Excellence for Nanoscale BioPhotonics (CE140100003 to E.M.G. and M.R.H.), UNSW Biomedical Engineering Seed Fund to G.L., and the National Natural Science Foundation of China (Grant 21575045) to G.L., Macquarie University MQRDG to G.L. and the Heart Research Institute to S.P.C. and M.M.K..

AUTHOR CONTRIBUTIONS

G.L. and E.M.G. conceived and designed the experiments. G.L. carried out the preparation and characterization of OnCELISA and data analysis. E.M.G. performed the theoretical modeling of OnCELISA and data analysis. S.P.C., M.M.K., and C.B. designed and performed aortic cell extraction and data analysis. G.L. and A.G.A. obtained confocal images of cells. L.M.P. performed IL-6 mRNA expression staining and confocal images. S.F., G.L., and D.W.I. designed and made the single-cell wells. G.L. and K.Z. performed the characterization of capture antibodies on cell surfaces. M.H. and E.M.G. performed imaging analysis. M.R.H. provided guidance on cell type selection. G.L, E.M.G., S.C., and M.R.H wrote the manuscript. All authors reviewed and edited the manuscript.

DECLARATION OF INTERESTS

The authors declare that no competing interests.

Received: April 22, 2019
Revised: September 10, 2019
Accepted: September 12, 2019
Published: October 25, 2019

REFERENCES

Achard, S., Jean, A., Lorphelin, D., Amoravain, M., and Claret, E.J. (2003). Homogeneous assays allow direct" in well" cytokine level quantification. Assay Drug Dev. Tech. *1*, 181–185.

Ali, M.M., Kang, D.K., Tsang, K., Fu, M., Karp, J.M., and Zhao, W. (2012). Cell-surface sensors: lighting the cellular environment. Wiley Interdiscip. Rev. Nanomed. Nanobiotechnol. *4*, 547–561.

Beigi, R., Kobatake, E., Aizawa, M., and Dubyak, G.R. (1999). Detection of local ATP release from activated platelets using cell surface-attached firefly luciferase. Am. J. Physiol. Cell Physiol. *276*, C267–C278.

Betzer, O., Meir, R., Dreifuss, T., Shamalov, K., Motiei, M., Shwartz, A., Baranes, K., Cohen, C.J., Shraga-Heled, N., and Ofir, R. (2015). In-vitro optimization of nanoparticle-cell labeling protocols for in-vivo cell tracking applications. Sci. Rep. *5*, 1–11.

Bienvenu, J., Monneret, G., Fabien, N., and Revillard, J.P. (2000). The clinical usefulness of the measurement of cytokines. Clin. Chem. Lab. Med. *38*, 267–285.

Biosciences, B. Detecting intracellular cytokines in activated lymphocytes. https://www.bdbiosciences.com/documents/Detecting_Cytokines_Lymphocytes.pdf.

Brosterhus, H., Brings, S., Leyendeckers, H., Manz, R.A., Miltenyi, S., Radbruch, A., Assenmacher, M., and Schmitz, J. (1999). Enrichment and detection of live antigen-specific CD 4+ and CD 8+ T cells based on cytokine secretion. Eur. J. Immunol. *29*, 4053–4059.

Childs, B.G., Durik, M., Baker, D.J., and Van Deursen, J.M. (2015). Cellular senescence in aging and age-related disease: from mechanisms to therapy. Nat. Med. *21*, 1424–1435.

Deng, W., and Goldys, E. (2014). Analyst *139*, 5321–5334.

Fan, R., Vermesh, O., Srivastava, A., Yen, B.K.H., Qin, L.D., Ahmad, H., Kwong, G.A., Liu, C.C., Gould, J., Hood, L., et al. (2008). Integrated barcode chips for rapid, multiplexed analysis of proteins in microliter quantities of blood. Nat. Biotechnol. *26*, 1373–1378.

Foster, B., Prussin, C., Liu, F., Whitmire, J.K., and Whitton, J.L. (2007). Detection of intracellular cytokines by flow cytometry. Curr. Protoc. Immunol. *110*, 6.24.1–6.24.18.

Gurevich, K.G., Agutter, P.S., and Wheatley, D.N. (2003). Stochastic description of the ligand-receptor interaction of biologically active substances at extremely low doses. Cell Signal. *15*, 447–453.

Hafler, D.A. (2007). Cytokines and interventional immunology. Nat. Rev. Immunol. *7*, 423.

Han, Q., Bradshaw, E.M., Nilsson, B., Hafler, D.A., and Love, J.C. (2010). Multidimensional analysis of the frequencies and rates of cytokine secretion from single cells by quantitative microengraving. Lab Chip *10*, 1391–1400.

Herrera, V., Hsu, S.C.J., Rahim, M.K., Chen, C., Nguyen, L., Liu, W.F., and Haun, J.B. (2019). Pushing the limits of detection for proteins secreted from single cells using quantum dots. Analyst *144*, 980–989.

Holmes, P., and Al-Rubeai, M. (1999). Improved cell line development by a high throughput affinity capture surface display technique to select for high secretors. J. Immunol. Methods *230*, 141–147.

Jiang, Z., Le, N.D., Gupta, A., and Rotello, V.M. (2015). Cell surface-based sensing with metallic nanoparticles. Chem. Soc. Rev. *44*, 4264–4274.

Joensson, H.N., and Svahn, H.A. (2012). Droplet microfluidics-A tool for single-cell analysis. Angew. Chem. Int. Ed. *51*, 12176–12192.

Jung, T., Schauer, U., Heusser, C., Neumann, C., and Rieger, C. (1993). Detection of intracellular cytokines by flow-cytometry. J. Immunol. Methods *159*, 197–207.

Kenney, J.S., Gray, F., Ancel, M.H., and Dunne, J.F. (1995). Production of monoclonal antibodies using a secretion capture report web. Biotechnology *13*, 787–790.

Kulbe, H., Chakravarty, P., Leinster, D.A., Charles, K.A., Kwong, J., Thompson, R.G., Coward, J.I., Schioppa, T., Robinson, S.C., and Gallagher, W.M. (2012). A dynamic inflammatory cytokine network in the human ovarian cancer microenvironment. Cancer Res. *72*, 66–75.

Lacy, P., and Stow, J.L. (2011). Cytokine release from innate immune cells: association with diverse membrane trafficking pathways. Blood *118*, 9–18.

Lei, J., and Ju, H. (2012). Signal amplification using functional nanomaterials for biosensing. Chem. Soc. Rev. *41*, 2122–2134.

Liu, G.Z., Qi, M., Huchtinson, M., Yang, G.F., and Goldys, E.M. (2016). Recent advances in cytokine detection by immunosensing. Biosens. Bioelectron. *79*, 810–821.

Love, J.C., Ronan, J.L., Grotenbreg, G.M., van der Veen, A.G., and Ploegh, H.L. (2006). A microengraving method for rapid selection of single cells producing antigen-specific antibodies. Nat. Biotechnol. *24*, 703–707.

Manz, R., Assenmacher, M., Pfluger, E., Miltenyi, S., and Radbruch, A. (1995). Analysis and sorting of live cells according to secreted molecules, relocated to a cell surface affinity matrix. Proc. Natl. Acad. Sci. U S A *92*, 1921–1925.

Müller, G., Müller, A., Tüting, T., Steinbrink, K., Saloga, J., Szalma, C., Knop, J., and Enk, A.H. (2002). Interleukin-10-treated dendritic cells modulate immune responses of naive and sensitized T cells in vivo. J. Invest. Dermatol. *119*, 836–841.

Nicola, N.A. (1994). Guidebook to Cytokines and Their Receptors (A Sambrook & Tooze Publication at Oxford University Press).

Quinn, J., Gratalo, D., Haden, K., and Moon, J. (2008). Accurate multiplex cytokine assay developed with VeraCode® technology.

Rider, T.H., Petrovick, M.S., Nargi, F.E., Harper, J.D., Schwoebel, E.D., Mathews, R.H., Blanchard, D.J., Bortolin, L.T., Young, A.M., Chen, J.Z., et al. (2003). A B cell-based sensor for rapid identification of pathogens. Science *301*, 213–215.

Schenk, T., Irth, H., Marko-Varga, G., Edholm, L., Tjaden, U., and van der Greef, J. (2001). Potential of on-line micro-LC immunochemical detection in the bioanalysis of cytokines. J. Pharm. Biomed. Anal. *26*, 975–985.

Starr, M.E., Evers, B.M., and Saito, H. (2009). Age-associated increase in cytokine production during systemic inflammation: adipose tissue as a major source of IL-6. J. Gerontol. A Biol. Sci. Med. Sci. *64*, 723–730.

Stenken, J.A., and Poschenrieder, A.J. (2015). Bioanalytical chemistry of cytokines–A review. Anal. Chim. Acta *853*, 95–115.

Stow, J.L., Low, P.C., Offenhäuser, C., and Sangermani, D. (2009). Cytokine secretion in macrophages and other cells: pathways and mediators. Immunobiology *214*, 601–612.

Streeck, H., Frahm, N., and Walker, B.D. (2009). The role of IFN-gamma Elispot assay in HIV vaccine research. Nat. Protoc. *4*, 461–469.

Tibbe, A.G., de Grooth, B.G., Greve, J., Dolan, G.J., Rao, C., and Terstappen, L.W. (2002). Magnetic field design for selecting and aligning immunomagnetic labeled cells. Cytometry *47*, 163–172.

Turcanu, V., and Williams, N.A. (2001). Cell identification and isolation on the basis of cytokine secretion: a novel tool for investigating immune responses. Nat. Med. *7*, 373–376.

Whicher, J., and Evans, S. (1990). Cytokines in disease. Clin. Chem. *36*, 1269–1281.

Wilson, N.J., Boniface, K., Chan, J.R., McKenzie, B.S., Blumenschein, W.M., Mattson, J.D., Basham, B., Smith, K., Chen, T., and Morel, F. (2007). Development, cytokine profile and function of human interleukin 17–producing helper T cells. Nat. Immunol. *8*, 950–957.

Young, H.A. (2009). Cytokine multiplex analysis. In Methods in Molecular Biology: Inflammation and Cancer, *Vol. 511*, S.V. Kozlov, ed. (Humana Press), pp. 85–105.

Zhao, W., Schafer, S., Choi, J., Yamanaka, Y.J., Lombardi, M.L., Bose, S., Carlson, A.L., Phillips, J.A., Teo, W., and Droujinine, I.A. (2011). Cell-surface sensors for real-time probing of cellular environments. Nat. Nanotechnol. *6*, 524–531.

ISCI, Volume *20*

Supplemental Information

A Nanoparticle-Based Affinity Sensor that Identifies and Selects Highly Cytokine-Secreting Cells

Guozhen Liu, Christina Bursill, Siân P. Cartland, Ayad G. Anwer, Lindsay M. Parker, Kaixin Zhang, Shilun Feng, Meng He, David W. Inglis, Mary M. Kavurma, Mark R. Hutchinson, and Ewa M. Goldys

Supplementary Information

A nanoparticle-based affinity sensor that identifies and selects highly cytokine-secreting cells

Guozhen Liu, Christina Bursill, Siân P. Cartland, Ayad G. Anwer, Lindsay M. Parker, Kaixin Zhang, Shilun Feng, Meng He, David W. Inglis, Mary M. Kavurma, Mark R. Hutchinson, Ewa M. Goldys

Transparent Methods

Preparation of superparamagnetic fluorescent beads labeled with IL-6 detection antibody

Superparamagnetic beads (SPIO) were selected for conjugation with the IL-6 antibody (CCC). Carboxylated superparamagnetic iron oxide particles (SPIO, 1% solid, 10 mg/mL, ~0.9 µm, Bangs Laboratories, USA) incorporating Dragon Green fluorophore (ex480, em520), (1 mg) were dispersed in 1 mL of 100 mM MES buffer at pH 5.2. This dispersion was then mixed with 3.2 mg EDC (1-ethyl-3-[3 dimethylaminopropyl]carbodiimide hydrochloride, Thermo Scientific) and 1.8 mg NHS (N-hydroxysuccinimide) and vortexed at room temperature for 30 min. After which the pH was adjusted to 8.0. The 20 µL anti-IL-6 monoclonal antibody catalog No. MAB406 from R&D Systems (0.5 mg mL^{-1} in 1xPBS) was added to the solution immediately, and stirred on a nonmagnetic mixing device for 2 h at room temperature. The resulting antibody-beads conjugates were magnetically separated by placing a magnet under the bottom of the reaction vessel, and the supernatant was discarded. Finally, the antibody modified SPIO (SPIO_Ab) was separated and washed with washing buffer (0.1 M 10xPBS, pH7.4) three times. The obtained SPIO_Ab was redispersed in 0.5 mL PBS and stored at 4 ^{o}C. The ratio equates to 10 µg antibody per mg beads. The same protocol was used for making superparamagnetic fluorescent beads labeled with IL-1β detection antibody except replacing anti-IL-6 monoclonal antibody by anti-IL-1β monoclonal antibody.

Sample preparation for confocal imaging and fluorescence staining

Cells were imaged using a SP2 (Leica Microsystems) confocal microscope. Cells were harvested after two washes with PBS, then pelleted at 1200 g for 5 min. Cells were then suspended in PBS at a density of 10^6 cells/mL. Cells were placed on 35 mm dishes with coverglass bottoms and allowed to settle for 10 minutes; other than this settling they remained suspended during imaging. Hoechst 33342 (H3570, Life Technologies, Australia) 5 µg/ml was used for nucleus staining. Cell Mask Deep Red (C10046, Life Technologies Australia) 5 mg/ml was used for membrane staining. For each group of control and treated cells. Spectral images were collected at 405-nm excitation wavelength and detected in 430-470 nm emission range for Hoechst and at 633 nm excitation wavelength and emission at 650-690 nm for Cell Mask Deep Red. FITC and Dragon Green was detected using 488 nm excitation and 520-560 nm

emission range. Phase contrast images were collected for all groups. All samples were imaged at the same parameters of pinhole aperture and detector voltage.

Cell biotinylation and conjugation of neutravidin

Two T75 cm^2 flasks of 90-95% confluent cells (10^7 cells each flask) were prepared. Cells were harvested at a density of 8.5-10 × 10^6 cells/mL and a volume of 1 mL of cell solution was suspended in 5 mL media. The cells were labelled with biotin using the protocol described in Pierce® Cell Surface Protein Isolation Kit (CAS No. PIE89881, Thermo Fisher Scientific). Specifically, the media was removed and cells were washed twice with 8 mL of ice-cold PBS per flask. The PBS was removed within 5 s. After that, 10 mL of the ice-cold biotin solution (1 mg mL^{-1}) was added to each flask, which was then placed on a rocking platform to gently agitate for 30 minutes at 4°C to ensure even coverage of the cells with the biotinylation solution. 500 µL of quenching solution was added to each flask to quench the reaction and the flask was gently tipped back and forth to ensure even coverage of the solution. The cells were gently scraped using the cell lifter into solution. The contents of two flasks were transferred to a single 50 mL conical tube. Both flasks were finally rinsed with a single 10 mL volume of tris-buffered saline (TBS) pH 7.2 and then the rinse volume was added to the transferred cells in the conical tube. Cells were centrifuged at 200 rcf for 6 min and supernatant was discarded. Cells were re-dispersed in PBS at cell density of ~10^6 cells/mL.

The 4 µg neutravidin (Thermo Fisher Catalog number 31000) was added to each 1 mL of cell solution. To the cell pellet, 5 mL TBS was added and cells were gently pipetted up and down twice with a serological pipette, which were centrifuged at 200 rcf for 6 min and supernatant was discarded. The obtained cells were collected for the antibody attachment as described below.

OnCELISA labelling

The biotinylated cells with neutravidin added (10^6 cells) were resuspended in 1 mL of gelatinous medium (25% gelatin) containing 2 µg biotinylated mouse anti-IL-6 goat IgG4 (CAS No. BAF406 from R&D Systems) (0.5 mg mL^{-1} in 1 × PBS) for 2 h at 37 ^oC. Then the cells were washed twice in 25 mL PBS, pH 7 and the cell pellets were collected. Cells were resuspended in 1 mL of 37^oC gelatinous medium (25% gelatin). After having been exposed to cytokines (either spiked into the medium, or secreted upon cell stimulation DG SPIO_IL-6_Ab

(10 μL per each 1 mL of cell solution at 10^6 cells/mL) was added to the medium and allowed to bind. After 1 h, the cells were washed 2 times with 1 × PBS.

Calibration curve of OnCELISA for detection of cytokines

The BV2 cells were prepared with the capture antibody conjugated on the cell surface according to the above OnCELISA protocol. Cell pellets were collected and cells were divided into 1 mL tubes at cell density of 10^6 cells/mL. Recombinant mouse IL-6 (CAS No.: 406-ML) at different concentration (from 0 to 1000 pg/mL) was externally added into individual tubes. Each concentration was spiked into 3 tubes to provide triplicate assay readings at that concentration. After waiting for 10 min, the cells from each tube were washed 2 times with 1 × PBS, and dispersed in 1 mL medium. The OnCELISA protocol was then completed, by adding DGSPIO_IL-6_Ab (10 μL) to the medium and this labelled detection antibody was then allowed to bind for 1 h. After this time, the cells were washed 2 times with 1 x PBS. Finally, the cells from each tube were dispersed in 1 mL PBS for fluorescence reading by using Fluorolog Tau-3 from Jobin-Yvon-Horiba. The results are plotted in Figure S3 b as average and standard deviation of the triplicate readings at each concentration.

Sample preparation for ELISA

BD OptEIA^{Tm} Mouse IL-6 ELISA kit (CAS No. 550950, BD Bioscience, Australia) was used to measure the concentration of IL-6 secreted by cells after LPS stimulation. For preparation of IL-6 samples, the biotinylated cells with the density of 10^6 /mL were suspended in 1 mL of warm medium containing 100 ng mL^{-1} LPS from Escherichia coli 026:B6 (Sigma Aldrich, Australia) to secrete IL-6 for 0 h, 2 h, 4 h, 6 h, 8 h, and 20 h, respectively. Supernatants from cells were collected in duplicate, and analysis was performed according to the manufacturer's instructions. For control measurements, IL-6 samples secreted by the original cells (without any functionalisation) were also prepared. All tests were performed using Nunc MaxiSorp 96 well plates, supplied with the ELISA Kit. BMG FLUOstar Galaxy Microplate Reader was used to measure absorbance at 450 nm. Optical density was also measured at 570 nm for wavelength correction. Results are analyzed and reported as means ± standard deviation.

Magnetic sorting

A magnetic sorter PickPen (Luoyang Huier Nani Science and Technology Co. LTD) was used to sort the cells labelled with fluorescent magnetic particles. In order to demonstrate

magnetic sorting, two suspensions of cells labeled with particles were prepared. One suspension was washed by using a normal protocol by centrifugation and cell strainer separation. Another suspension was washed by the application of magnetic pen in cell suspension for 1 min, and then the tip of magnetic pen was released in a clean tube and washed with PBS. Then the washed cells were collected for confocal imaging.

Size and zeta potential measurement

The hydrodynamic size and the zeta potential of the magnetic nanoparticles before and after conjugations with the antibody were determined using Zeta Sizer Nano Series Nano-ZS (Malvern Instrument, UK).

Fluorescent *in situ* hybridization

Primers for fluorescent *in situ* hybridization (FISH) were designed using Primer3 (NCBI Nucleotide), spanning exon-exon junctions and including the functional protein coding region of the mouse IL6 mRNA sequence (NCBI accession NM 031168). The forward primer includes the SP6 promoter sequence (ATTTAGGTGACACTATAGAAG) at the 5' end while the reverse primer includes the T7 promoter sequence (TAATACGACTCACTATAGGGAGA) at the 5' end. IL6 F Primer with SP6 at 5' end: 5'ATTTAGGTGACACTATAGAAG-GGGACTGATGCTGGTGACAA 3'; R Primer with T7 at 5' end: TAATACGACTCACTATAGGGAGA-TAACGCACTAGGTTTGCCGA. Standard PCR was performed for IL6 mRNA using mouse BV2 cell cDNA, the resulting PCR product transcribed was from bp 76 to bp 674 (599bp total length) of the mouse IL6 mRNA sequence. In each 25 µL reaction tube: 12.5 µL AmpliTaq Gold® 360 Master Mix (Life Technologies), 1 µL Forward Primer, 1 µL Reverse Primer, 1 µg cDNA, 9.5 µL RNAse/DNAse free water. Additionally, no template control and no primer control reactions were run in parallel for comparison to IL6 PCR product. Tubes were held at 95°C for 10 min to activate the Taq enzyme followed by 40 cycle repeats of 95°C 30 sec (denaturation), 60 °C 30 sec (annealing), 72 °C 60 sec (extension) and a final extension at 72 °C for 7 min. PCR products were purified using a column extraction kit according to the manufacturer protocol (PureLink® PCR Purification Kit; Life Technologies). PCR products were then run on a 2% TAE gel containing SYBR Gold and photographed on a Genesnap gel doc (Syngene) to confirm appropriate molecular weight and the absence of primer dimer.

Purified IL-6 PCR product was *in vitro* transcribed to complimentary RNA strands using the MEGAscript® T7 Transcription Kit (AM1334; Life Technologies) according to the manufacturer protocol using 200 ng of PCR product from each gene. Biotin-UTP and biotin-CTP were incorporated into the IL6 cRNA probe. Sense IL6 control strands were *in vitro* transcribed using the MEGAscript® SP6 Transcription Kit (AM1330; Life Technologies) according to the manufacturer protocol. All RNA probes were purified with $LiCl_2$ solution, washed with EtOH, air dried and reconstituted in 40 µL of RNAse/DNAse free water. RNA probe quality and quantity was then assessed using a Nanodrop 2000 spectrophotometer (NanoDrop Technologies, Wilmington, DE, USA). RNA probes were run on a denaturing formaldehyde gel with MOPS buffer using electrophoresis to confirm molecular weight and specificity.

BV2 cells were treated with LPS (1.0 µg mL^{-1} concentration) in 2 ml of their normal DMEM on coverslips in 6 well plates. LPS in DMEM was removed immediately and replaced with PBS pH 7.2 for 0 h LPS treatments. Cells inside the manufactured microchip, or on coverslips were first washed in PBS pH 7.2 and fixed using 4% formaldehyde for 10 min and then again washed with PBS. They were permeabilised with 70% EtOH for 30 min at 4 ^{O}C then washed with PBT solution (PBS + 0.01% Tween-20). Pre-hybridization buffer (50% formamide, 5 × SSC pH 7.0, 250 µg mL^{-1} herring sperm DNA, 5% dextran sulfate, 1X Denhardt's solution, 0.1% Tween-20) was added to cells with 1000ng of cRNA probe and incubated for ~16hrs in an incubator at 37 ^{O}C. Cells were washed 3x in 2X SSC buffer (sodium citrate/NaCl solution) followed by 3 × washes in PBT solution. Samples were incubated for 1hr at room temp (~22 ^{O}C) with 2.5 µg of streptavidin-Alexafluor647 or streptavidin-Alexafluor555 (Molecular Probes, Life Technologies). Cells were then washed 3 × 5 minutes in PBT solution on an orbital shaker. Cells stained on coverslips or microchips were mounted onto slides in Prolong Gold Antifade Media with DAPI dye (P 36931, Life Technologies) and photographed with wide field (Zeiss Axioimager Z1) or confocal microscopy (Leica Microsystems SP2).

ImageJ (http://rsb.info.nih.gov/ij) was used for FISH analysis on slides. Data were calculated at a threshold of 10% maximum brightness intensity. All data is presented as mean ± SEM. Data was compiled and graphed using Graphpad Prism software (Version 6.07). Student's t-test was used for statistical analysis between treatments where $p<0.05$ was considered significant.

Fabrication of SU-8 molds and PDMS chips with single cell wells

The procedure was based on Reference [1]. The entire array of single cell wells was designed to be 40.00 mm long and 0.90 mm wide. It had a rectangular array of 25 μm diameter pillars also 25 μm apart, 900 pillars along the array, 18 pillars across the array. Using this layout pattern, 20-μm thick SU-8 master molds were created on 3" wafers using standard photolithography processes. An intermediate glass-supported PDMS (Sylgard 184 prepolymer) mold was created from the SU-8 master. This intermediate was then treated with a 430 mtorr oxygen plasma and silanized by soaking in isopropyl alcohol containing 1% OTS (octadecyltrichlorosilane) for 15 min. The same PDMS prepolymer was then poured onto the intermediate mould and cured at 65℃. The final PDMS substrate was peeled off. It had 25 μm diameter holes and 25 μm hole-to-hole gaps, and it was abricated with depth of each hole of 20 μm. Furthermore, the PDMS substrate was diced to create single rectangular microchip units with 27 holes in one direction) and 18 holes in the perpendicular direction. The 2.5 mL microcentrifuge tubes were filled with 1.5 mL of PDMS, which was cured. The diced PDMS pieces containing wells were placed in the tubes and glued into place with the wells facing up. These tubes were then treated with OTS (as above) to reduce non-specific adhesion. Following a rinsing with isopropyl alcohol the tubes containing single-cell-wells were ready to use.

Placing single cells in wells

The microchip was mounted perpendicularly inside a 1.5 mL in an Eppendorf tube. The cell solution 50 μL at cell density of 2×10^6/mL was placed in the tube and centrifuged for 5 minutes at 1500 rpm. This made it possible for cells to be placed individually in the wells. After the application of OnCELISA in single cells in wells, the mounted microchip was taken out from the tube and placed on a petri dish for confocal microscopy imaging.

Animal study protocol

Mice were bred at the Heart Research Institute Sydney, Australia. Protocols were approved by the Sydney Local Health District Animal Ethics Committee (2014-014) (Sydney, Australia). Six-week-old atherosclerosis-prone male apolipoprotein $E^{-/-}$ mice were fed standard chow for 16 weeks to develop atherosclerotic plaque in their aortic arches and descending thoracic aortae. Two hours prior to euthanasia by cardiac exsanguination, mice were injected with LPS (100 μg/mouse) or PBS i.p. Aortae were excised. Single cell suspensions were prepared from the

aortic tissue using an enzymatic digestion containing Collagenase I and Collagenase IX (both from Sigma Aldrich) and then passage through a cell strainer (70 µm). Cells were subjected to the OnCELISA using antibodies raised against mice (anti-IL-6 monoclonal antibody). Cells were subjected to flow cytometry on a BD FACSVerse (BD Biosciences) and the data was analysed using FlowJo® software.

Statistics

One-tailed t-test was performed for the investigated groups of animals in the atherosclerosis study. The test was applied by using software Prism. The level of statistical significance was set at $p < 0.05$

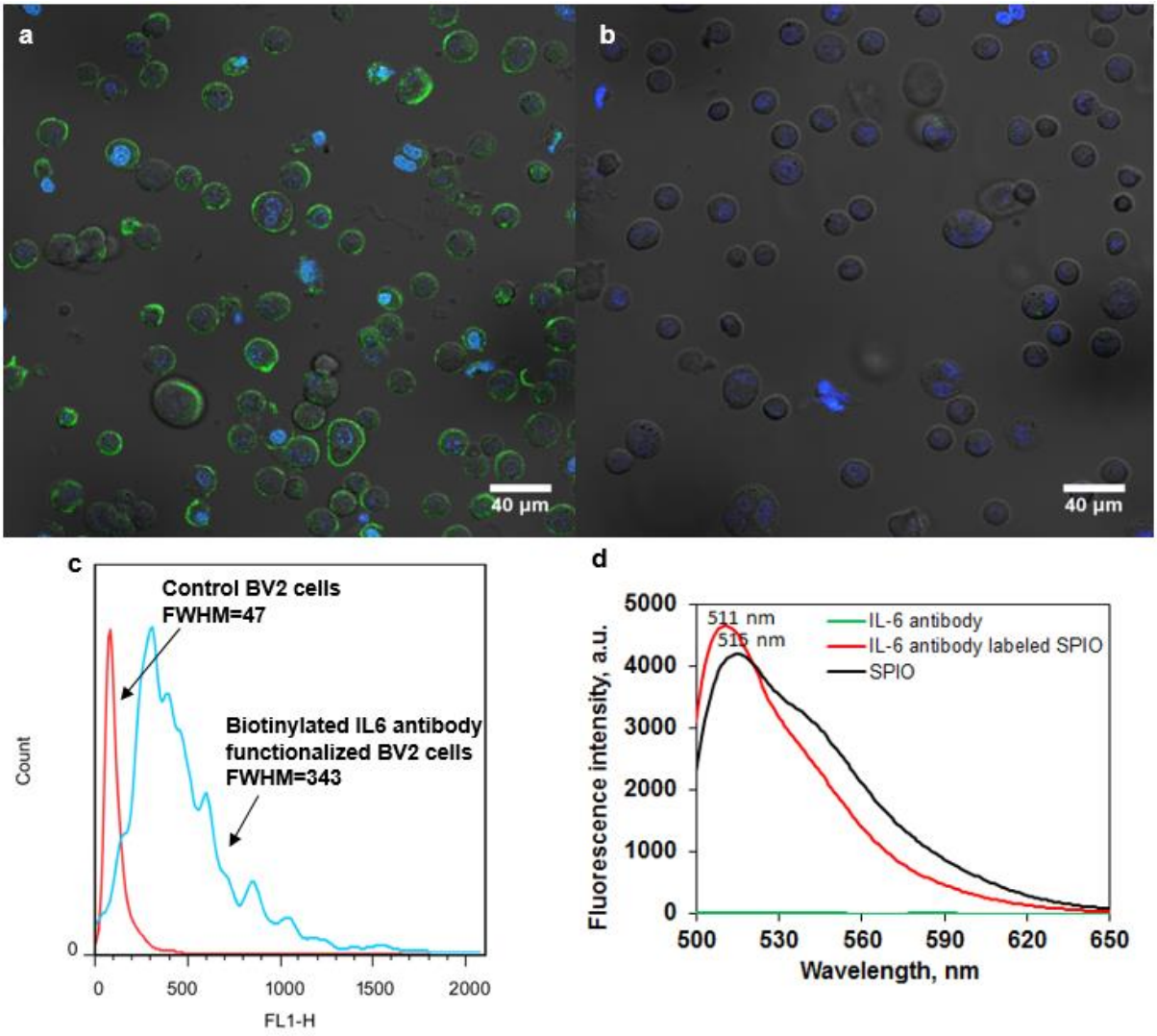

Figure S1. Demonstration of the localization of the capture antibody and detection when combined with fluorescent magnetic beads (SPIO). a) Confocal image of the IL-6 capture antibody in BV2 cells after treatment with FITC labeled secondary antibody. Image has been combined with a DIC image of the same field of view. b) Confocal image of BV2 cells that have not been incubated with the capture antibody, after treatment with FITC labeled secondary antibody (negative control). Image has been combined with a DIC image of the same field of view. c) Flow cytometry histograms for control BV2 cells (without the capture antibody, red line) and IL-6 capture antibody-modified BV2 cells after treatment with FITC labeled secondary (blue line). d) The fluorescence spectra for IL-6 only (green line), IL-6 + SPIO (red line) and SPIO only (black line). The Dragon Green magnetic particles (SPIO), IL-6_Ab, + SPIO_IL-6_Ab were excited at 480 nm. Related to Figure 1.

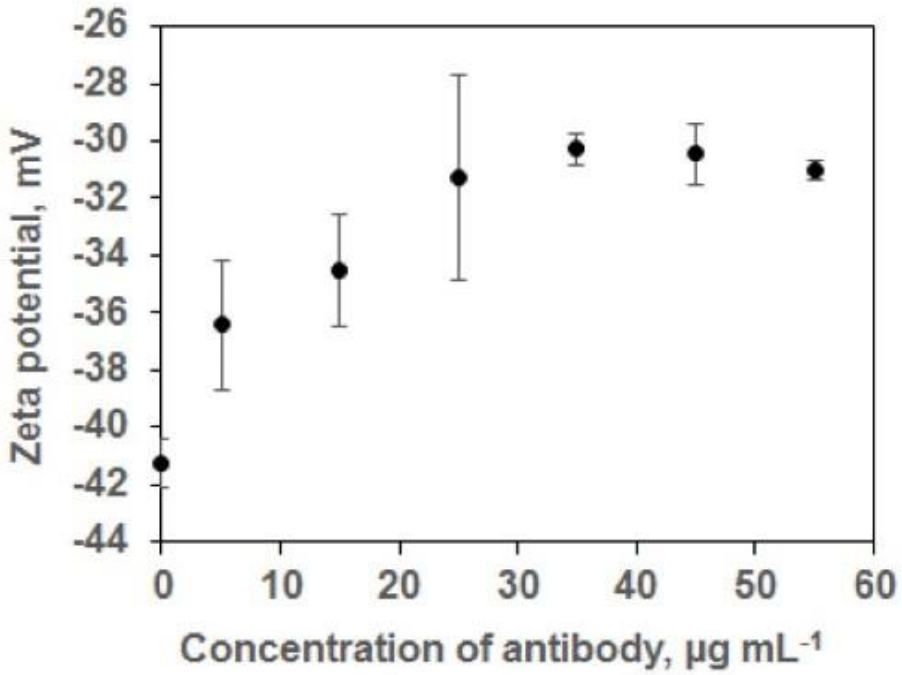

Figure S2. Confirmation of antibody attachment to magnetic nanoparticles. The zeta potential for magnetic nanoparticles before (0 µg/mL) and after conjugation of IL-6 antibodies at different concentrations. The zeta potential decreases with the increase in IL-6 antibody concentration reaching a plateau at 8 µg mL^{-1}. Related to Figure 1.

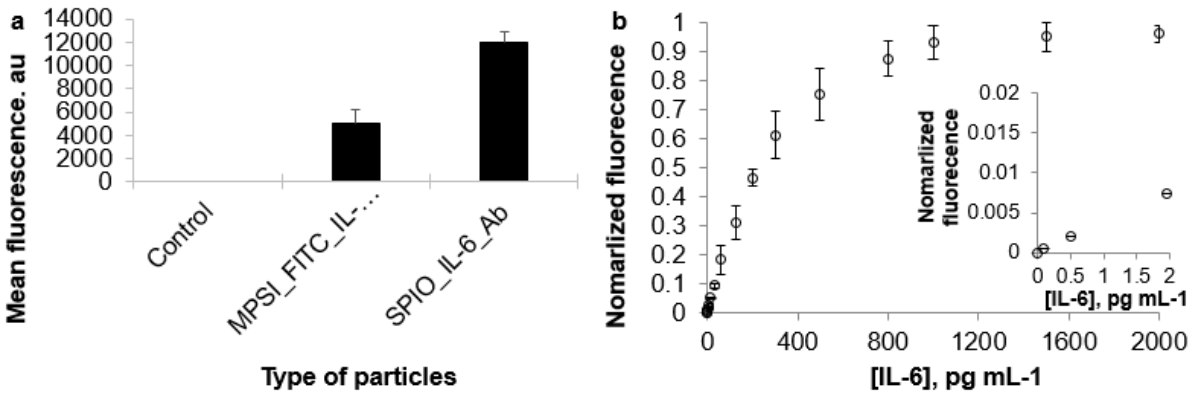

Figure S3. a) The affinity of the IL-6 antibodies conjugated to DG SPIO_IL-6_Ab and to MPSi_FITC_IL-6_Ab determined by the fluorescence plate reader. In this experiment IL-6 (200 pg mL^{-1}) was added to 96 well plate followed by adding MPSi_FITC_IL-6_Ab or DG SPIO_IL-6_Ab, and finally, the wells were washed 5 times with PBS. The ELISA Plate reader (BMG FLUOstar Galaxy-Multi-functional Microplate Reader) was used to detect fluorescence (excitation at 492 nm). The DG SPIO_IL-6_Ab particles show a stronger fluorescence signal than the MPSi_FITC_IL-6_Ab. b) Sensitivity and linear range of the OnCELISA assay (functionalized cells with the capture antibody on the surface incubated with DG SPIO_IL-6_Ab particles as the detection antibody). Based on the calibration curve of IL-6 shown in b) the low detection limit is 0.1 pg mL^{-1} and the linear range of the assay is 0.1-1000 pg mL^{-1}. Note that this low detection limit was obtained with fluorimetry readout, and the corresponding low detection limit using microscopy is different (higher). Related to Figure 1.

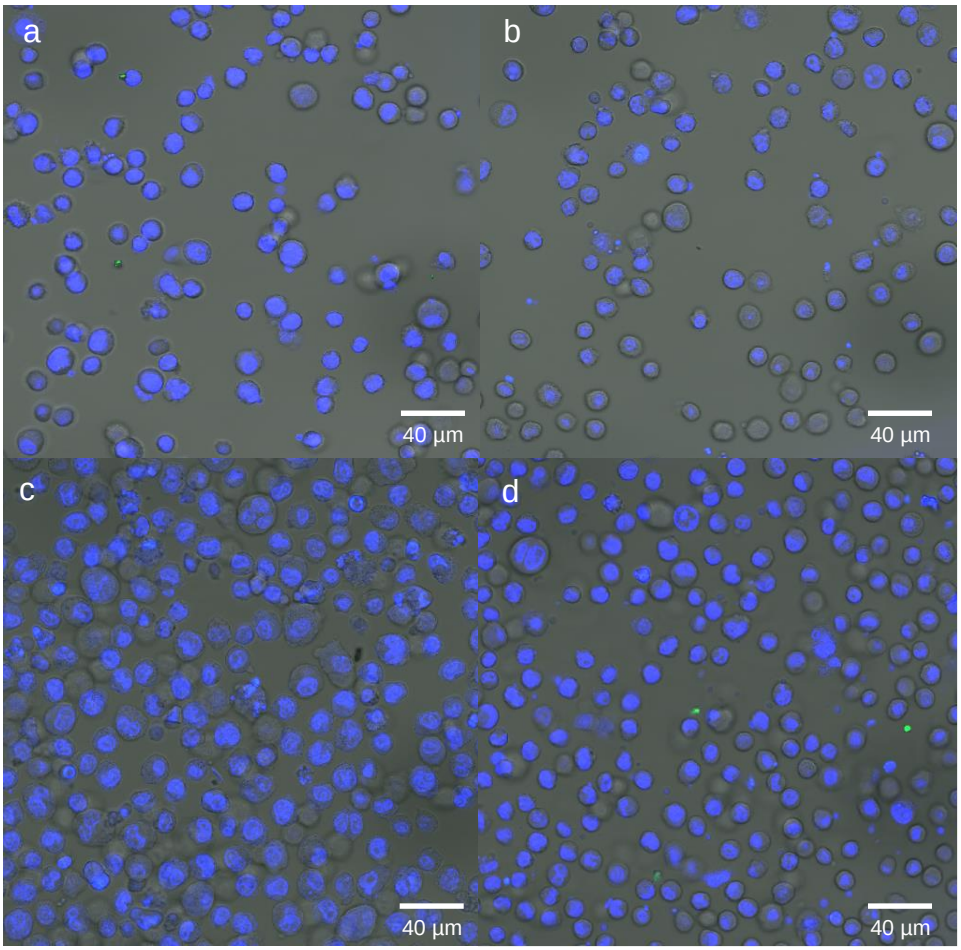

Figure S4. Systematic control experiments confirming the importance of each constituent of the OnCELISA. Confocal laser scanning microscopy images combined with DIC images for control samples (blue is Hoechst nucleus staining, DG SPIO nanoparticles are shown in green). The following controls were carried out: a) Biotinylated BV2 cells were treated with DG SPIO_IL-6_Ab, without neutravidin. The results demonstrate only very low (< 5%) non-specific adsorption of nanoparticles on biotinylated cell surfaces or nanoparticle uptake. b) Biotinylated BV2 cells were treated with neutravidin, and then DG SPIO_IL-6_Ab after LPS stimulation to verify that the presence of biotinylated anti_IL-6_Ab is vital to the function of the prepared affinity surface. c) Biotinylated BV2 cells were treated with neutravidin, a biotinylated mismatched antibody (anti IL-1β_Ab), and then with DG SPIO_IL-6_Ab after LPS stimulation. d) Biotinylated BV2 cells were treated with neutravidin, biotinylated anti_IL-6_Ab, and then DG SPIO with a mismatched anti-chicken Ab after LPS stimulation (labelled with Alexa Fluor® 488 conjugate) to establish the selectivity of the prepared capture surfaces. Related to Figure 1.

Table S1. Details for all control experiments. Related to Figure 4.

	Components of OnCELISA assay					
	OnCELISA results	**Biotinylation**	**Neutravidin**	**Biotinylated anti IL-6 Ab**	**IL-6**	**DG SPIO_IL-6_Ab**
Control 1	Negative	Yes	No	No	Yes	Yes
Control 2	Negative	Yes	Yes	No	Yes	Yes
Control 3	Negative	Yes	Yes	Yes, but replaced by DG SPIO_IL-1β_Ab	Yes	Yes
Control 4	Negative	Yes	Yes	Yes	Yes	Yes, but replaced by DG SPIO_anti-chicken_Ab

Table S1 details for control experiments to validate the components of the OnCELISA assay. The results show that there is negligible non-specific adsorption of nanoparticles on biotinylated cells. In addition, almost no labelling was observed when the biotinylated anti-IL-6 capture antibody was not modified on the cell surfaces, suggesting that the capture antibody is very important to the function of the affinity surface. No fluorescence was observed after functionalized cells were treated with the fluorescent detection antibody anti-chicken IgG which has no affinity to IL-6, suggesting that the capture surface is selective to IL-6. All these controls suggest that the cells labelling is due to the affinity between IL-6 antibody and the IL-6 secreted by cells, and not to non-specific adsorption or uptake.

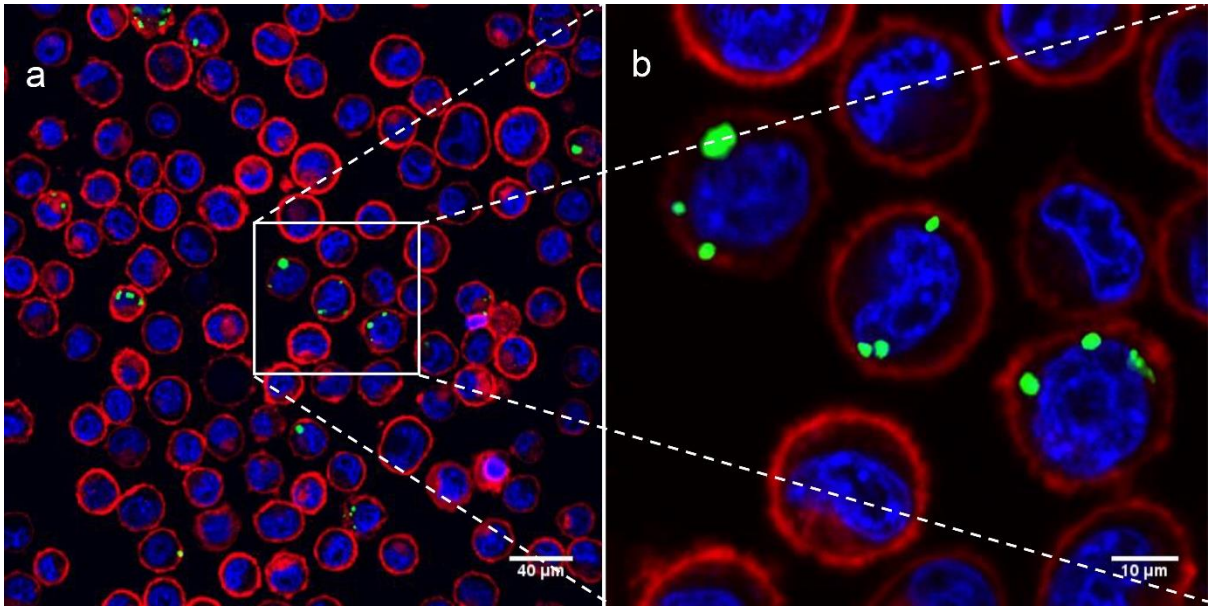

Figure S5. Confocal images for BV2 cells after treatment with OnCELISA (green) combined with nuclear (blue) and membrane (red) staining (a) at lower magnification; (b) at higher magnification. Related to Figure 1.

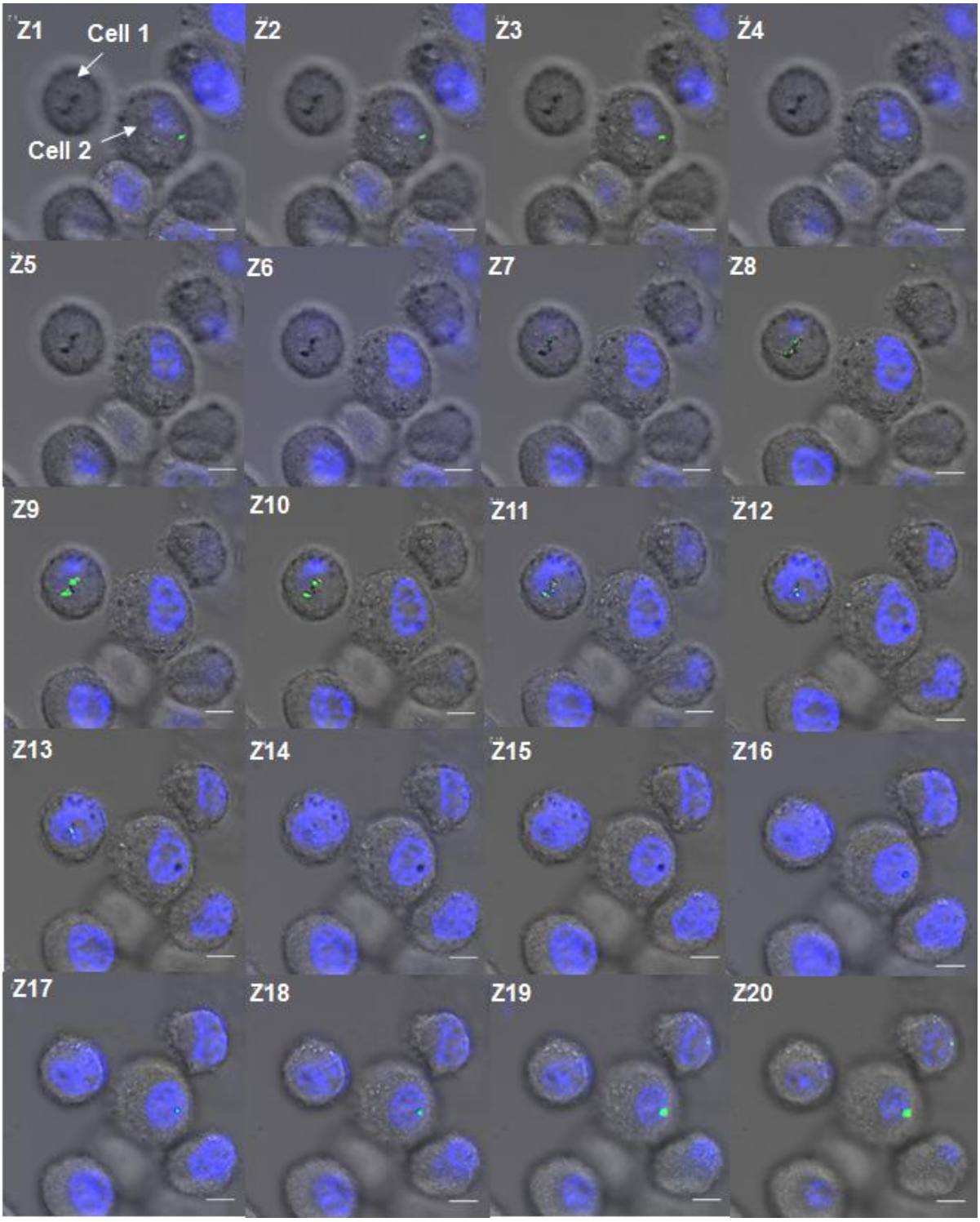

Figure S6. Consecutive Z-stack images showing the location of of OnCELISA labelling. In this figure confocal images have been combined with DIC images of the same field of view. Z-separation of individual images is 1.05 um. Upon inspection of consecutive images Z-1 through to Z-9 we can see Cell 1 slowly coming into focus. The image plane significantly intersects the cell nucleus on images Z-11 to Z-19, with maximum cross-section around image Z-15, marking the approximate center of the cell. In contrast, the OnCELISA labeling on Cell

1 is brightest in the Image Z-9, consistent with labeling on the top or bottom of the cell. Similar effect is seen in Cell 2 where OnCELISA labeling is observed at the beginning and at the end of the presented Z-stack, where the cell cross-section seems to be out-of focus, but the nucleus seems the biggest around the middle of the stack. Scale bar = 10 μm. Related to Figure 1.

Vesicular model of cytokine release

The below section is to formulate a mathematical model the process of cytokine release and determine its impact on chemical kinetics of the OnCELISA immunoassay. We intend to establish whether OnCELISA on an individual cell detects its own cytokines, secreted from that particular cell or whether it detects cytokines secreted from adjacent cells. To this aim, we calculate the fraction of the cell-bound Abs in the OnCELISA assay that are able to detect its own molecules (akin to autocrine detection), secreted by this particular cell and self-captured. We consider a vesicular release mechanism of cytokines[2], which produces short bursts of locally high cytokine concentrations.

Cytokines are released from immune cells via diverse pathways, some of which involve secretory vesicles [2]. In our model A we assume that the IL-6 is released from spherical secretory vesicles with radius $r_{vesicle}$ that are below the optical diffraction limit ($r_{vesicle}$ =0.1 um) and that the concentration of IL-6 in such vesicles, $N_{vesicle}$ is high ($N_{vesicle}$= 10 mM, see **Table S2** for summary of all numerical values used in these calculations). Once cytokines are released from the vesicle, they form a hemispherical cloud of molecules with an average concentration $C_{released}(t)$. In the case of diffusion in free space away from a molecular source, the average square distance of molecules from the source over time t is Dt where *D* is the diffusion constant. Therefore, the radius of the hemispherical cloud is $R = \sqrt{Dt}$. In our simplified model we assume that the released molecules form a uniform density hemispherical cloud of this radius. The background cytokines produced by other cells are also present, with a uniform low concentration, C_b. The total concentration of cytokines available for binding in the cytokine cloud is $C(t) = C_{released}(t) + C_b$, and outside it is C_b. C_b is generally small compared to $C_{released}(t)$ on the timescale of single seconds considered here. In this case the released average cytokine density in the proximity of the cell surface can be approximated by:

$$C(t) = \frac{1}{2} N_{vesicle} \left(\frac{r}{(Dt)^{1/2}} \right)^3 \qquad /1\text{-}1/$$

Estimates of relevant physical constants

Estimate of diffusion constant of IL-6 in water and in gelatin solutions. In experimental protocols for cell-surface assays, gelatin may be used to slow down diffusion[3]. In this section we estimate the diffusion constant of IL-6 in the media containing water, 25% gelatin, and 40% gelatin respectively. To estimate this diffusion constant we used the approach in Reference[4]. IL-6 is assumed to be a spherical molecule [4]. The diffusion of spherical molecules is given by the Stokes-Einstein equation:

$$D = \frac{k_B T}{6\pi\eta r} \qquad /1\text{-}2/$$

where T is the absolute temperature in Kelvins, r is the Stokes radius of the spherical molecule and η is the viscosity of the solvent at the experiment temperature, in [Pa s], k_B is the Boltzmann constant. The Stokes radius is a function of molecular weight and between 4 kDa and 40 kDa and it varies from 2 nm to 6.5 nm [4]. IL-6 has 24 kDa on average with 4 close forms with 22 to 26 kDa, therefore we have taken r = 5 nm to be the Stokes radius of IL-6.

Viscosity values in gelatin solutions. Here we estimate the viscosity of gelatin solutions, featuring in the Stokes equation. The intrinsic viscosity $[\eta]$ defined as the ratio of specific viscosity η_{sp} to *c*, the concentration of polymer in grams per 100 cm^3 in the limit of small *c* is between 40 and 80 cm^3/g,[5] and is usually equal to the ratio of $[\eta] = \frac{\eta_{sp}}{c}$ [5]. The specific viscosity is obtained from relative viscosity as η_r as

$$\eta_{sp} = \eta_r - 1 \qquad /1\text{-}3/$$

while relative viscosity is the ratio of the viscosity of the solution to that of the solvent.

Using the value of $[\eta]$ = 50 cm^3/g and the concentration of gelatin, *c* = 25 g/100 cm^3 (25 % gelatin) we get

$\eta_{sp} = [\eta]c = 12.5$, $\eta_r = 13.5$. Using the value of viscosity of water of 0.8 mPa s [6] we obtain the viscosity of 25% gelatin η =10.8 mPa s. We remind that Pa = N/m^2.

For *c* = 40 g/100 cm^3 (40% gelatin) we obtain η = 16 mPa s. Substituting into Equation /1-2/ we get $D = 4 * 10^{-8}$ cm ^{2}/s for 25% gelatin and $D = 2.5 * 10^{-8}$ cm^2/s for 40% gelatin. These values can be compared with the diffusion constant for Il-6 in water of $2.7 * 10^{-7}$ cm^2/s [7], and for GFP in water of $8.7 * 10^{-7}$ cm^2/s reported in Reference.[4]

Table S2. Values of parameters used in the mathematical modeling.

Quantity	Value	Reference
v_{sample}	1 cm^3	n/a
n_{cells}	10^6	n/a
ρ	10 μm = 10^{-3} cm	n/a
$N_{vesicle}$	10 mM	n/a
$r_{vesicle}$	0.1 um	n/a
D	$2.5 * 10^{-8}$ cm^2/s	Our estimates, see above, for 40% gelatin
∇T	$0.25 * 10^3$s	Francis, K.; Palsson, B. O. *Proceedings of the National Academy of Sciences* **1997**, *94*, 12258.

Analysis of chemical kinetics. The interaction of cytokines released from the vesicles is further described in terms of a chemical reaction framework through capture antibody and cytokine concentrations, kinetic rates, and binding affinity. In respect to binding kinetics, we adapt here the model presented in Reference [8]

IL-6 binding to antibodies on the cell surface is described in terms of the effective on-rate K_{on} and off-rate k_{off}. The number of antibody-IL-6 bonds per unit area, $N(t)$ satisfies the relationship [8]:

$$\frac{dN(t)}{dt} = K_{on}[N_{max} - N(t)] - k_{off}N(t) \qquad /1\text{-}4/$$

Here, N_{max} is the maximum number of bonds given by the antibody density per unit cell area. The on-rate K_{on} is a lumped kinetic constant $K_{on} = k_{on} * C(t)$ where k_{on} is the on-rate per antibody molecule (in units of $(Ms)^{-1}$). The equation has the solution:

$$N(t) = \frac{K_{on}N_{max}}{K_{on}+k_{off}}\{1 - exp[-(K_{on} + k_{off})]\}, \qquad /1\text{-}5/$$

or substituting for K_{on}:

$$N(t) = \frac{C(t)k_{on}\,N_{max}}{C(t)k_{on}+k_{off}}\{1 - exp[-(C(t)k_{on} + k_{off})]\} \qquad /1\text{-}6/$$

Numerical estimates of binding kinetics. We now estimate the bond density. To this aim, we note that the antibodies used here had the affinity constant $\frac{k_{on}}{k_{off}}$ in the order of 10^{11} M^{-1} [9] . The parameter k_{off} is taken to be in the range of 10^{-5} s^{-1} to 10^{-4} s^{-1} [10]. Correspondingly, k_{on} is in the range of 10^6 -10^7 $(Ms)^{-1}$. In the limit of large cytokine concetrations discussed here the contribution from k_{off} is negligible and $N(t)$ can be approximated by:

$$N(t) \approx N_{max}\{1 - exp[-(C(t)k_{on})]\} \qquad /1\text{-}7/$$

The bond density increases exponentially with a time constant τ such that $\tau^{-1} = C(\tau)k_{on}$. In particular, substantial, 63% (63%=$\left[1 - \frac{1}{e}\right]$) antibody binding is achieved after time τ and higher percentage binding is achieved for longer times. We now estimate this time constant for our estimated cytokine concentration..

$$\tau = \frac{1}{C(\tau)k_{on}} = \frac{2}{k_{on}N_{vesicle}} \left(\frac{(D\tau)^{1/2}}{r_{vesicle}}\right)^3, \qquad /1\text{-}8/$$

Or, solving for τ

$$\tau = \frac{(k_{on}N_{vesicle})^2 {r_{vesicle}}^6}{4D^3} \qquad /1\text{-}9/$$

Substituting the values for 25% gelatin and taking k_{on} = 10^6 - 10^7 $(Ms)^{-1}$, $N_{vesicle}$=10 mM and vesicle radius $r_{vesicle}$=0.1 μm and *D*= 4 $\mu m^2/s$ we obtain: $\tau_{0.25} =$ 0.4 s and this >63% binding will take place in the region of radius $(D\tau)^{1/2}$=1.25 μm. For 40% gelatine we obtain $\tau_{0.4} =$ 1.59 s and this >63% binding will take place in the region of radius $(D\tau)^{1/2}$=1.99 μm.

Conclusions: Can OnCELISA detect cytokines from other, non-secreting cells by the virtue of their proximity to a secreting cell? With the assumptions of our model we now answer the question whether there is cross-labeling from a secreting cell to other, potentially non-secreting cells. Our calculations indicate that the cytokines from any adjacent cell whose secreting vesicle is closer to the selected cell than the diffusion distance of 1.25 μm (25% gelatin) and 2 μm (40% gelatin) will be able to attach to the antibodies at the adjacent cell and saturate the bonds to 63% - which means that the adjacent cell will be labelled despite being non-secreting. However, this is a relatively rare occurrence and the labelling of the non-secreting cell touching only 1 secreting cell will remain very low. Simple geometry considerations indicate that two spherical cells 10 um diameter and touching one another have

a small percentage (4.8%) of their area closer than 2 μm to one another (and correspondingly less for 1.25 μm diffusion distance). Labelling of the non-secreting cell would require the appearance of the secreting vesicle in the secreting region immediately adjacent to the non-secreting cell, and the number of such vesicles would be proportional to the area ratio (that is scaled down by a factor of 4.8%). This means that even if the vesicle would eventually be present within the appropriate area, the non-secreting cell would only be able to be labelled in the small area representing 4.8% of the cell area. The situation becomes less clear-cut in the case when there is a larger fraction of highly secreting cells. In the case of a single non-secreting cell that is surrounded by closely packed secreting cells in the hcp lattice where each cell has 12 neighbors, over 50% of the area of the non-secreting cells could, in principle be labelled. This may set a limit on the purity of cell subpopulations selected by using OnCELISA, but it could be partially moderated by setting comparatively high gating limits in flow cytometry sorting.

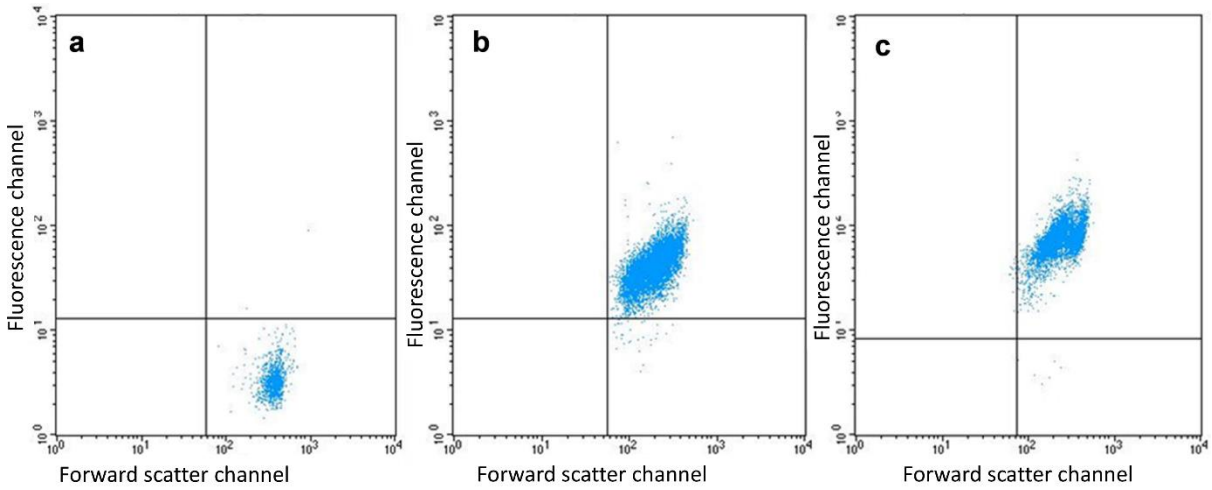

Figure S7. The progeny cells of biotinylated BV2 cells are also biotinylated. (a) control BV2 cells; (b) biotinylated BV2 cells; (c) progeny of biotinylated BV2 cells. The cells were stained with FITC-avidin before flow cytometry measurement. Related to Figure 4.

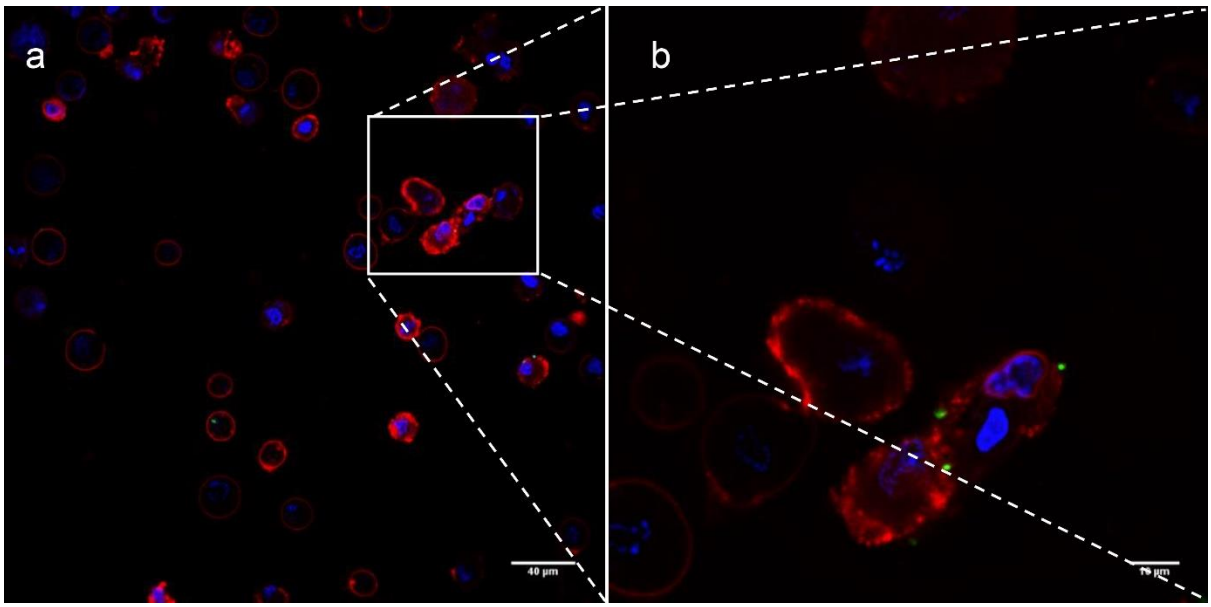

Figure S8. OnCELISA applied to mesenchymal stem cells (MSCs). (a-b) Confocal laser scanning microscopy images for mesenchymal stem cells (MSCs) which have been labeled with DG SPIO_IL-6_Ab at different magnifications. Related to Figure 1.

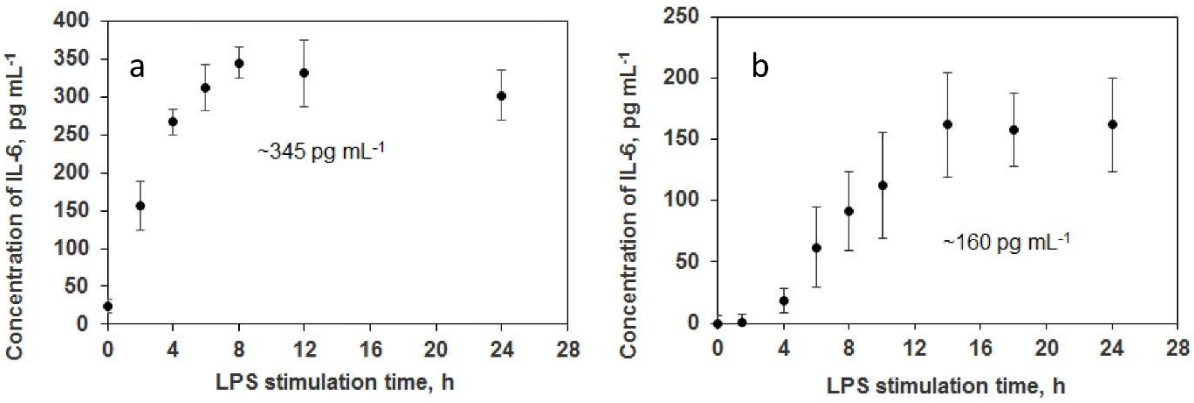

Figure S9. ELISA measurements of IL-6 secreted from RAW cells (a) and MSCs (b). Related to Figure 1.

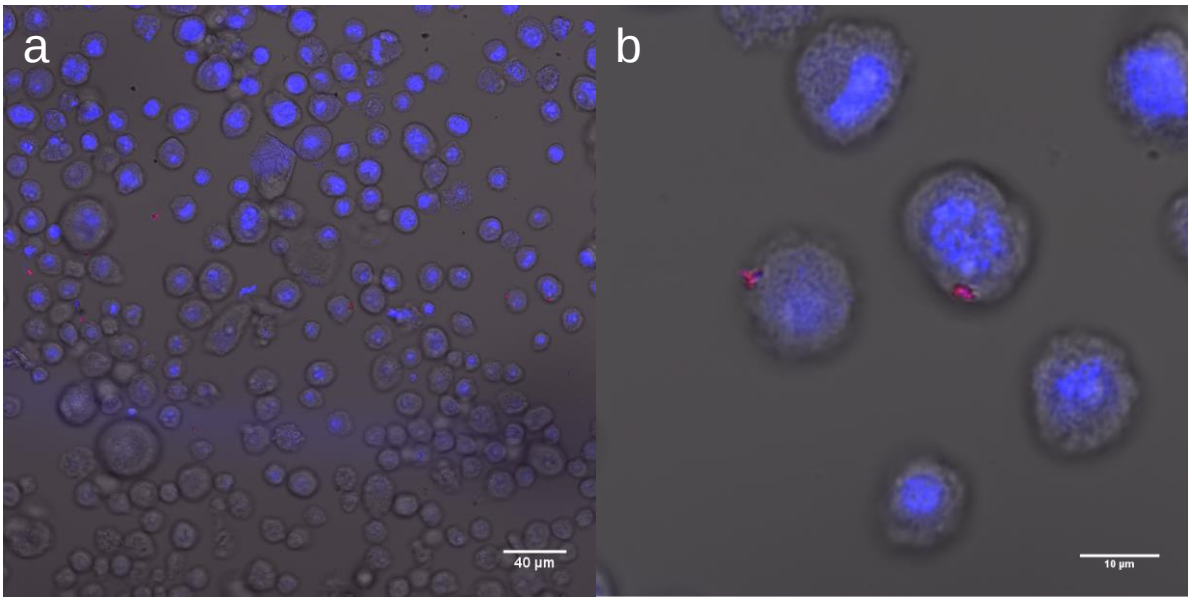

Figure S10. OnCELISA can detect the secretion of IL-1β. Confocal laser scanning microscopy images combined with DIC images for functionalized cells with 8 h LPS stimulation after treatment with Flush Red SPIO_IL-1β_Ab at different magnifications. Related to Figure 1.

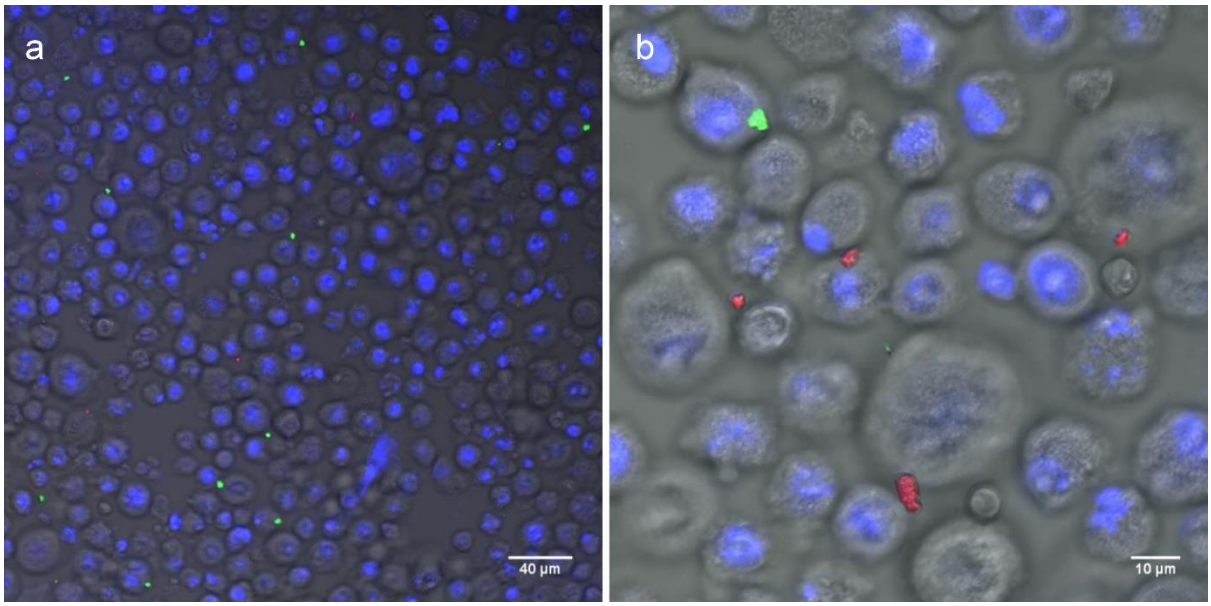

Figure S11. OnCELISA can be simultaneously used with two different colour nanoparticles and two cytokines, IL-6 and IL-1β. Confocal laser scanning microscopy images have been combined with DIC images of the same field of view. Images show functionalized cells with 8 h LPS stimulation after treatment with DG SPIO_IL-6_Ab and flush red SPIO_IL-1β_Ab at different magnifications. Related to Figure 1.

References

1. Huang, L., Chen, Y., Chen, Y.F. & Wu, H.K. Centrifugation-Assisted Single-Cell Trapping in a Truncated Cone-Shaped Microwell Array Chip for the Real-Time Observation of Cellular Apoptosis. *Anal. Chem.* **87**, 12169-12176 (2015).
2. Lacy, P. & Stow, J.L. Cytokine release from innate immune cells: association with diverse membrane trafficking pathways. *Blood* **118**, 9-18 (2011).
3. Manz, R., Assenmacher, M., Pfluger, E., Miltenyi, S. & Radbruch, A. Analysis and sorting of live cells accordig to secreted molecules relocated to a cell-surface affinity matrix. *Proc. Natl. Acad. Sci. U.S.A.* **92**, 1921-1925 (1995).
4. Kihara, T., Ito, J. & Miyake, J. Measurement of Biomolecular Diffusion in Extracellular Matrix Condensed by Fibroblasts Using Fluorescence Correlation Spectroscopy. *Plos One* **8**(2013).
5. Masuelli, M.A. Hydrodynamic Properties of Gelatin –Studies from Intrinsic Viscosity Measurements. in *Products and properties of biopolymers* 85-116 (Verbeek C.J.R. , 2012).
6. https://en.wikipedia.org/wiki/Viscosity.
7. Goodhill, G.J. Diffusion in axon guidance. *Eur. J. Neurosci.* **9**, 1414-1421 (1997).
8. Li, B., Chen, J. & Long, M. Measuring binding kinetics of surface-bound molecules using the surface plasmon resonance technique. *Anal. Biochem.* **377**, 195-201 (2008).
9. Green, N.M., Anfinsin, C.B., Edsall, J.T. & Richards, F. *Adv. Protein Chem.*, (Academic Press, San Diego,CA, 1975).
10. Kusnezow, W., Syagailo, Y.V., Goychuk, I., Hoheisel, J.D. & Wild, D.G. Antibody microarrays: the crucial impact of mass transport on assay kinetics and sensitivity. *Expert Rev. Mol. Diagn.* **6**, 111-124 (2006).